DOI: 10.1002/chem.200701769

Schiff Base Macrocycles Containing Pyrroles and Pyrazoles

Stamatia Katsiaouni,[a] Sebastian Dechert,[a] Raymond P. Briñas,[b, c] Christian Brückner,*[b] and Franc Meyer*[a]

Abstract: A double nucleophilic substitution reaction of 3,5-bis(chloromethyl)pyrazole with pyrroles generates a novel pyrrole–pyrazole hybrid building block, the pyrazole analogue to tripyrrane. Vilsmeier–Haack formylation produces the corresponding dialdehyde, which was used in the formation of a series of nonaromatic Schiff base macrocycles. NMR and UV/Vis spectroscopy and single-crystal diffractometry were used to characterize the novel macrocycles. The solid-state structures of select free bases and protonated members of this class of macrocycles display a range of intra- and intermolecular hydrogen-bonding patterns that suggest their use in molecular-recognition systems. They also contain an acid-sensitive chromophore. Their acid–base and anion-recognition properties were ascertained; alas, only modest anion-selective spectroscopic signatures could be detected by using UV/Vis and ^{1}H NMR spectroscopy. The macrocycles proved resistant toward oxidation to their aromatic congeners. The pyrrole–pyrazole building blocks presented are potentially useful for the synthesis of a range of pyrazole analogues of all-pyrrole macrocycles.

Keywords: hydrogen bonds · macrocycles · pyrazoles · pyrroles · Schiff bases

Introduction

Aromatic as well as nonaromatic macrocyclic oligopyrrolic compounds, together with their acyclic counterparts, have been the subject of many studies.[1] Select members of these structurally diverse classes have attracted special attention in past years due to their rich coordination and anion-recognition chemistry.[2] Among them, macrocycles incorporating Schiff base-type linkages are particularly popular.[3,4,5] The popularity of Schiff base compounds is derived from their relative ease of formation and the presence of a basic imine functionality, which offers an additional coordination or hydrogen-bonding site. Representative nonaromatic Schiff base pyrrole-based compounds with rich anion- and cation-binding properties are compounds **1** and **2**, introduced by Love et al. and Katayev, Sessler et al., respectively.[6,7]

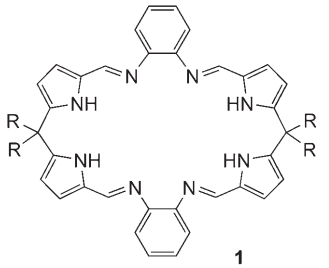

1

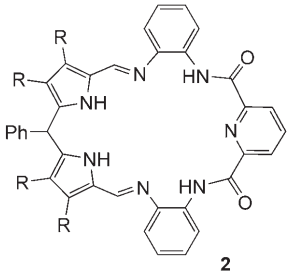

2

[a] Dr. S. Katsiaouni, Dr. S. Dechert, Prof. Dr. F. Meyer
Institut für Anorganische Chemie
Georg-August-Universität
Tammannstrasse 4, 37077 Göttingen (Germany)
Fax: (+49) 551-393063
E-mail: franc.meyer@chemie.uni-goettingen.de

[b] Dr. R. P. Briñas, Prof. Dr. C. Brückner
Department of Chemistry
University of Connecticut
Unit 3060, Storrs, CT 06269-3060 (USA)
Fax: (+01) 860-486-2981
E-mail: c.bruckner@uconn.edu

[c] Dr. R. P. Briñas
Current address: Department of Biology
Brookhaven National Laboratory, Upton, NY (USA)

Supporting information for this article is available on the WWW under http://www.chemeurj.org/ or from the author.

The use of pyrazole moieties (or other heterocycles such as triazoles) in linear and macrocyclic compounds is much less developed than that of pyrroles. Nonetheless, several interesting multidentate cyclic and linear ligands have become known. Prototypic for this class is macrocycle **3**, which has been intensely investigated by the groups of Navarro and García-España.[8] Pyrazoles combine hydrogen-bond donor and acceptor capabilities into the same functionality.[9] Furthermore, pyrazoles are very useful building blocks in bioinorganic coordination chemistry because they offer a reasonable compromise for mimicking the bridging carboxylate donors found in nature.[10] Like carboxylates, they are monoanionic donors supporting a range of metal–metal distances, but unlike carboxylates, they can be incorporated much more readily into compartmentalized ligand frameworks. These aspects make pyrazoles particularly interesting for incorporation into molecular-recognition systems and biomimetic bimetallic complexes.[8,10,11,12]

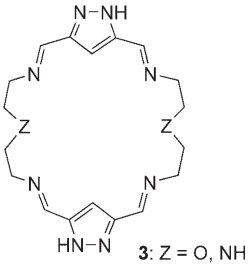

3: Z = O, NH

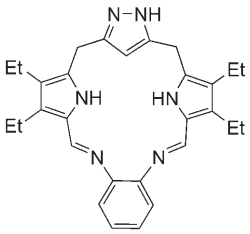

4a

Although a combination of pyrroles and pyrazoles into one ligand framework suggests itself, prior to our recent communication reporting macrocycle **4a**,[13] little was known about such compounds.[14] We attribute the scarcity of information on pyrazole-containing pyrrolic macrocycles to the absence of suitable pyrazole-based building blocks.

We will disclose here the details of the synthesis of the key pyrrole–pyrazole building block, and its application in the synthesis of a family of pyrrole–pyrazole-containing macrocycles (**4**).[13] The acid–base properties of these compounds are discussed and the scope and limits of these macrocycles in molecular-recognition events are ascertained by using single-crystal diffractometry, and UV/Vis and NMR spectroscopy. As will become evident, the novel macrocycles do not compete, at least not as far as tested, with the anion-recognition abilities of many other pyrrole-based macrocycles. However, the novel compounds are expanding the range of readily accessible and potentially useful oligopyrrolic macrocycles, and they feature a unique combination of hydrogen-bonding donor and acceptor sites.

Results and Discussion

Retrosynthetic analysis of macrocycles of type 4: As the first example of a pyrrole–pyrazole hybrid Schiff base macrocycle we decided to synthesize macrocycles of type **4**, the retrosynthetic analysis of which is shown in Scheme 1. Schiff base reaction of any 1,2- (or, perceivably, wider spaced) diamine **I** with dialdehyde **5** likely generates the macrocycle,

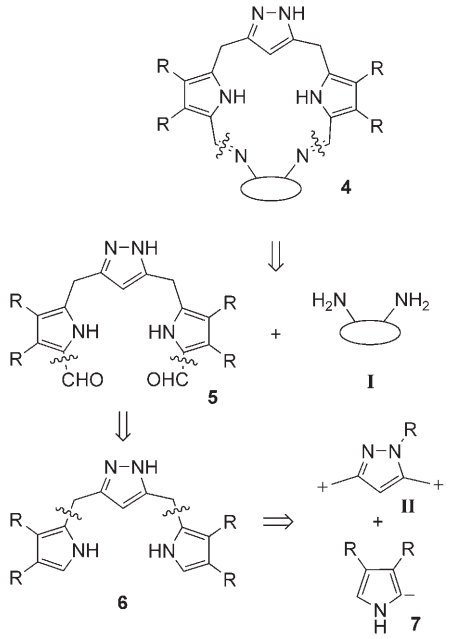

Scheme 1. Retrosynthetic analysis of target macrocycle **4**.

with the 3,5-bis(pyrrol-2-ylmethyl)-substituted pyrazoldialdehyde **5** being identified as the key intermediate. This dialdehyde is perceivably accessible by Vilsmeier–Haack formylation of **6**, itself the reaction product of pyrazole synthon **II** and an appropriately activated pyrrole. Several N-protected and unprotected derivatives suitable as synthon **II** are known, among them the tetrahydropyranyl (THP)-protected and the unprotected chloro- and bromomethyl derivatives.[15,16,17] This reaction sequence is essentially the pyrazole analogue of the ring-closing step in the synthesis of sp^3-texaphyrin **13** (see below, Scheme 5).

Formation of the 3,5-bis(pyrrol-2-ylmethyl)pyrazoles: Based on precedent substitution reactions from our laboratories involving THP-protected 3,5-bis(halomethyl)pyrazole (**8**),[15,17] we reacted this compound with pyrrole under a range of basic conditions (Grignard pyrrole, *n*BuLi) (Scheme 2).

We quickly realized that forcing conditions (several equivalents of *n*BuLi) were required to accomplish the desired substitution reaction, irrespective of whether the chloro (**8a**)[16,17] or bromo (**8b**) derivative [15] were used (Scheme 2). Even under forcing conditions, the isolated yield of the desired bis(pyrrol-2-ylmethyl)-substituted pyrazole **10** was unsatisfactory (17%), and the monosubstitution product **9** was generally present in larger quantities (29%). Worse than the low yields, however, was the circumstance that we were not able to deprotect the pyrazole moiety in **10** using the traditional acidic conditions (i.e., dry ethanolic HCl)[17,18] without extensive decomposition of **10**.

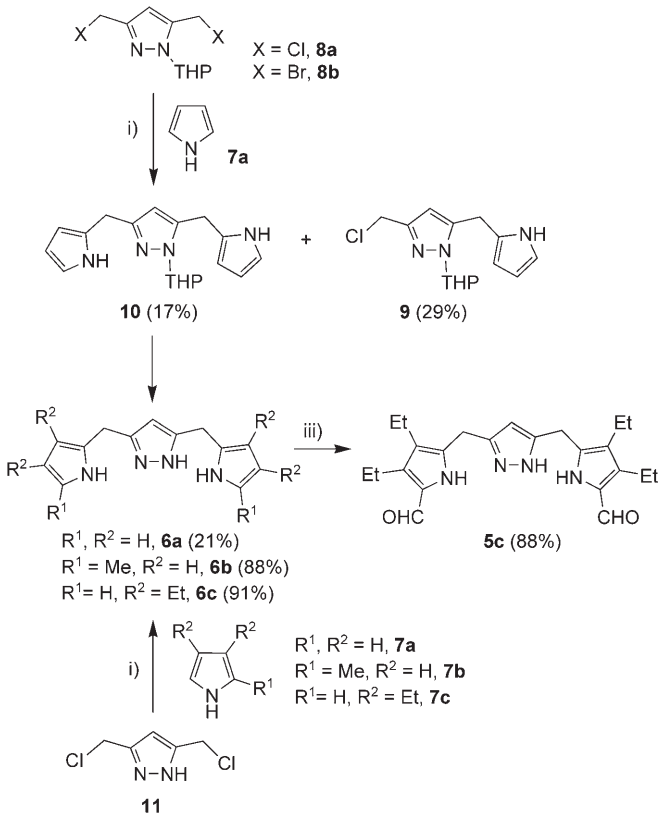

Scheme 2. Reaction conditions: i) 1) pyrrole (4 equiv), *n*BuLi (4 equiv), CH_2Cl_2 or THF (dry), −30 °C, N_2 atm, 1.5 h; 2) 15 h, RT; 3) saturated aq NH_4Cl; 4) column chromatography. ii) 1) *n*BuLi (3.5–4.0 equiv), CH_2Cl_2 (dry), −78 °C, N_2 atm, 4 h; 2) 15 h, RT; 3) saturated aq NH_4Cl; 4) column chromatography. iii) 1) DMF (dry; 10 equiv), benzoyl chloride (8 equiv), 0 °C for 2 h, then warming to RT, 4 h; 2) ethanolic Na_2CO_3; 3) column chromatography.

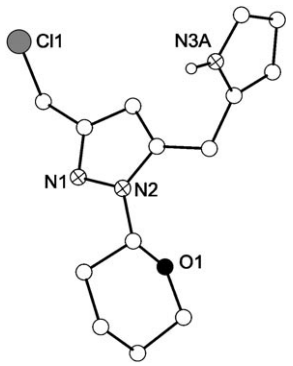

Figure 1. View of the molecular structure of **9**. All CH hydrogen atoms and the disorder of the pyrrole have been omitted for clarity.

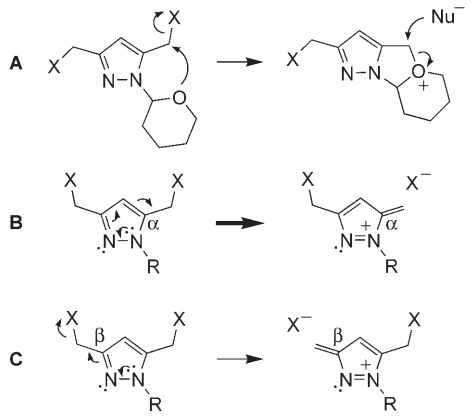

Scheme 3. Mechanistic rationalization of the observed reactivity of **8**.

Monosubstitution took place selectively at the chloromethyl group adjacent to the nitrogen atom carrying the THP group and not, as could have been assumed based on steric grounds, at the chloromethyl group on the opposite side. The structural assignment of **9** was confirmed by using X-ray diffraction (Figure 1).

We have observed a similar reactivity pattern before.[19] Several possible mechanistic explanations for this observation that find some parallels in the chemistry of pyrrole can be offered (Scheme 3).

Anchimeric assistance of the tetrahydropyrane oxygen atom may assist in the substitution reaction (mechanism **A**), but only the chloromethyl group adjacent to the THP group is susceptible to this activation effect. Additionally, the observed degree of selectivity reflects the electronic influence of the lone pair of the THP-substituted amine-type nitrogen atom on the halomethyl substituent attached at its α position (**B**), as compared to its β position (**C**). Inversely, it reflects the unavailability of the lone pair of the imine-type nitrogen atom to assist in the nucleophilic displacement. This interpretation suggests the removal of the THP group from **8** prior to the substitution reaction. The absence of the protecting group in **11** removes the accelerating effect of the anchimeric assistance but allows rapid tautomeric exchange of the hydrogen atom between both nitrogen atoms, thus making the α/β reactivity differences obsolete. Hence, substitution at both halomethyl positions of **11** is expected, though perhaps combined with an overall slower rate of substitution.

Indeed, reaction of the unprotected pyrazole derivative **11** with pyrrole **7a** using a fourfold stoichiometric excess of base (*n*BuLi) generates the desired compound **6a**, albeit in modest yield (21%), and no significant quantities of the monosubstituted product were observed. A contributing aspect to the low isolated yield of **6a** is that, analogously to its all-pyrrole congeners, the tripyrranes, it is rather unstable.[20] Protection of the α positions of pyrrole moieties is a proven way of stabilizing oligopyrrolic compounds. Thus, reaction of **11** with 2-methylpyrrole (**7b**) produces **6b** in 88% yield. By using optimized reaction conditions, reaction of **11** with diethylpyrrole (**7c**) generates **6c** in 91% yield as an off-white solid. The ethyl substituents were introduced at the β positions to prevent attack at these positions in subsequent reactions and to assist in the solubility of the final products. Spectroscopic and analytical data confirm the identity of **6c**. For instance, diagnostic signals in the

^{1}H NMR spectrum of this pyrrole–pyrazole hybrid are the signal for the pyrazole moiety ($\delta = 5.88$ ppm, s, 1H) in combination with the signals for the α position of the diethylpyrrole ($\delta = 6.33/6.34$ ppm, s, 2H) and the methylene linkages ($\delta = 3.83$ ppm, s, 4H). This key intermediate can be made in multigram quantities though it is susceptible to (acid-catalyzed) decomposition and is best kept in the freezer and under an N_2 atmosphere.

Also analogously to its all-pyrrole analogues, Vilsmeier–Haack-type bisformylation of **6c** is possible, generating **5c** in good yields (88%).[21] Introduction of the formyl groups greatly stabilizes the compound, and **5c** can be kept for extended periods of time without decomposition. Among other things, the replacement of the α-pyrrole signals in the ^{1}H NMR spectrum of **6c** by aldehyde signals (at $\delta =$ 9.45 ppm) and the characteristic $\nu_{C=O}$ signal at 1608 cm^{-1} in the IR spectrum of **5c** define the identity of this product. The availability of this compound allowed us to proceed toward the target compounds. However, it should be noted that this compound is also a potential building block for a range of pyrazole analogues of pyrrolic (macrocyclic) compounds.

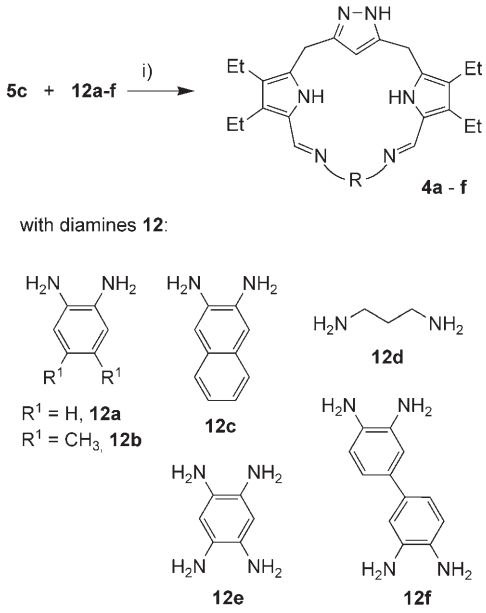

Scheme 4. Reaction conditions: i) 1) MeOH (dry), stoichiometric excess of TFA, N_2 atm, reflux, 20–30 h; 2) column chromatography.

Formation of pyrrole–pyrazole hybrid macrocycles 4a–4f: The Schiff base condensation reaction between a tripyrrane dialdehyde and a diamine is well known. Notably, when using diaminobenzenes this reaction generates the nonaromatic precursors to texaphyrins (sp^3-texaphyrins).[4,22] Analogously, the trifluoroacetic acid (TFA)-catalyzed reaction between pyrrole–pyrazole dialdehyde **5c** and a range of aromatic (**12a–12c**) and aliphatic (**12d**) diamines generates, after purification by using column chromatography over aluminum oxide followed by crystallization, yellow compounds in yields of up to 90% (at a 0.5 mmol scale) that can be characterized as the macrocycles **4a–4d**, respectively (Scheme 4). Purification of the macrocycles by crystallization in the absence of any basic conditions, including the absence of aluminum oxide, generates them as their TFA salts (**4**·TFA).

The composition of the reaction product between, for example, dialdehyde **5c** and diamine **12a**, was ascertained by using high-resolution mass spectrometry (HRMS, ESI+) to be $C_{29}H_{35}N_6$, the expected composition for the (monoprotonated) reaction product of the 1:1 condensation product **4a**. The ^{1}H and ^{13}C NMR spectra of products **4** demonstrate their twofold symmetry (fast tautomeric exchange interchanges the two nonequivalent pyrazole nitrogen atoms). The presence of diagnostic signals in the ^{1}H and ^{13}C NMR spectra for the 4-position of the 3,5-disubstituted pyrazole moiety (**4a**: $\delta = 5.67$ ppm, s, 1H; and $\delta = 103.9$ ppm, respectively), an imine functionality (**4a**: $\delta = 8.15$ ppm, s, 2H; and $\delta = 146.1$ ppm, respectively) together with a sharp imine band in the IR spectrum (**4a**: 1614 cm^{-1}), and characteristic signals for the amine backbone used, also suggest the formation of a macrocycle. In addition, the chemical shift for the methylene protons (**4a**: $\delta = 3.88$ ppm, s, 4H) indicate that the macrocycle does not contain a fully conjugated π system. Accordingly, the yellow color ($\lambda_{max} = 331$ nm for **4a**) of relatively low absorptivity ($\log \varepsilon_{331} = 4.37$) and the characteristics of the UV/Vis spectrum are not at all porphyrin-like (Figure 2). The macrocycles derived from the aromatic 1,2-amines (**4a–4c**) are stable solids that readily crystallize. Hence the structural assignments derived from the spectra could also be confirmed by single-crystal X-ray diffractometry of select members (see below). Macrocycle **4d**, derived from the aliphatic 1,3-diamine **12d**, is somewhat less stable and could not be crystallized.

Macrocycles **4a**,**b** are the pyrazole analogues of the macrocyclic, nonaromatic sp^3-texaphyrin **13**, the precursor to the aromatic expanded porphyrin texaphyrin **14** (Scheme 5).[4,22] However, in contrast to **13**, compounds **4a**,**b** have resisted, to date, all of our attempts of oxidizing them to a fully aromatic system (using 2,3-dichloro-5,6-dicyano-1,4-benzoquinone (DDQ), *p*-chloranil, $BaMnO_4$[23] or MnO_2, in the absence or presence of a range of metal ions and/or bases).[4,22] Pyrazole derivatives, owing to the presence of two electronegative nitrogen atoms, are known to be much less reactive than pyrroles toward electrophilic attack and oxidation.[9] Considering further the reported difficulties of oxidizing texaphyrinogen **13** to the metallated or free base fully aromatic analogue,[4,22] our inability of oxidizing **4a–c** to pyrazole analogues of texaphyrin is not altogether surprising (but still being investigated).

Reaction of the bis(1,2-diamines) **12e** and **12f** with **5c** also generated red-brown solids in high yields, which in solution gave spectroscopic signatures similar to those of, for instance, **4a** (and yellow solutions for the free bases). Analysis by using HRMS (ESI+) confirmed their composition corresponding to the expected bis-macrocycles **4e** and **4f**, respectively. However, their low solubility, especially of **4e**, has hampered their detailed study.

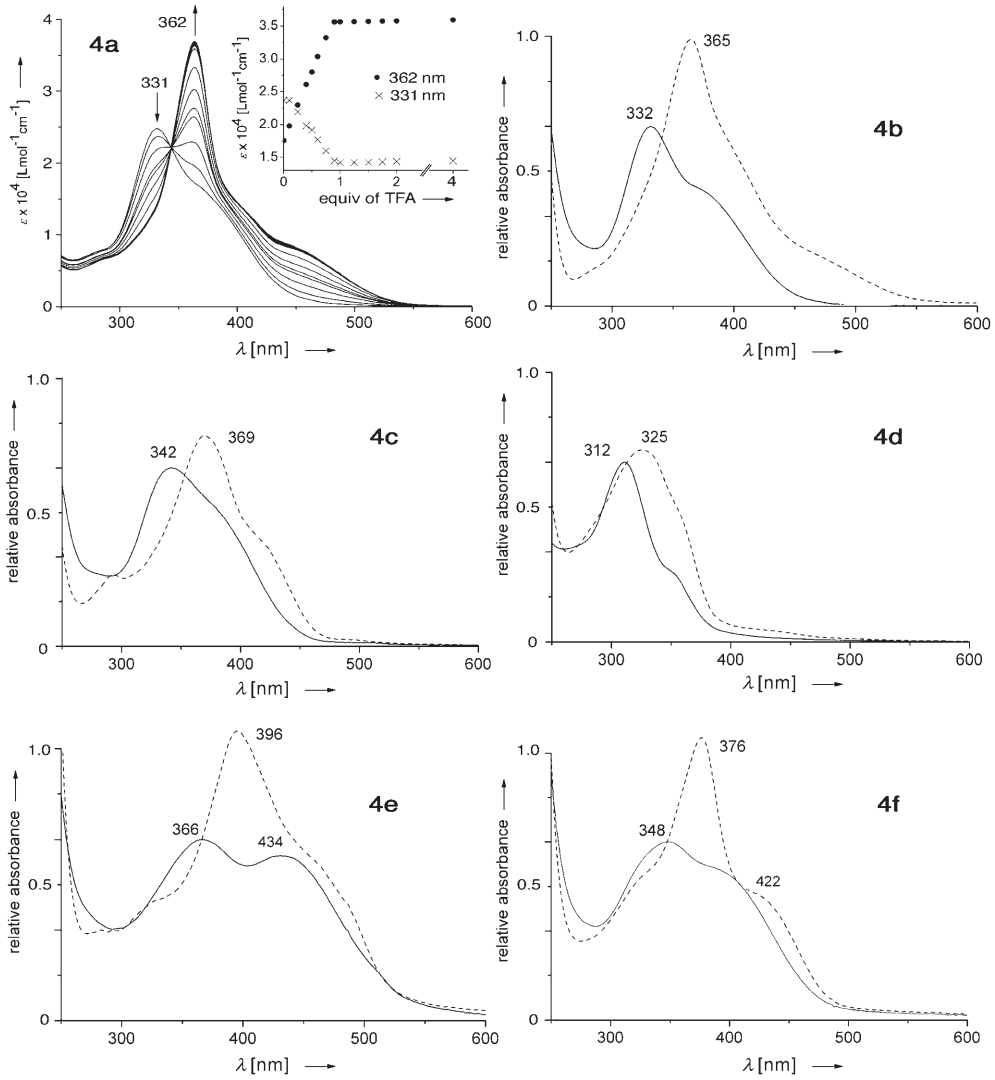

Figure 2. UV/Vis spectra of the Schiff base macrocycles indicated in 0.01 % Et_3N (——) and with excess TFA (-----) in $CHCl_3$. For **4a**: UV/Vis spectrophotometric titration of a solution of **4a** in $CHCl_3$ (4.2×10^{-5} M) with TFA (0.01 M in $CHCl_3$); inset: titration profile (molar absorbance ε at $\lambda = 331$ nm (×) and 362 nm (●) versus equivalents of TFA).

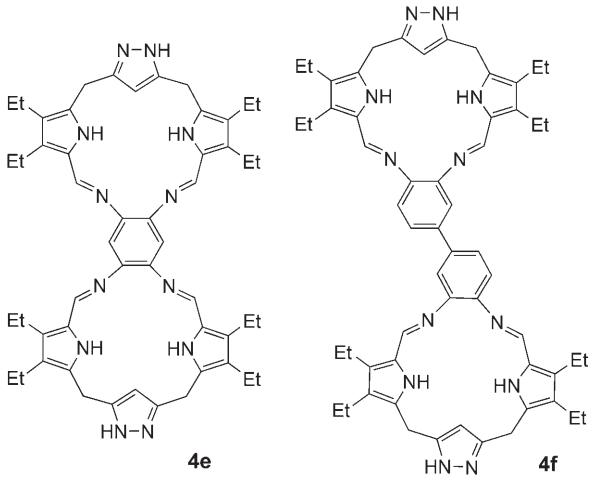

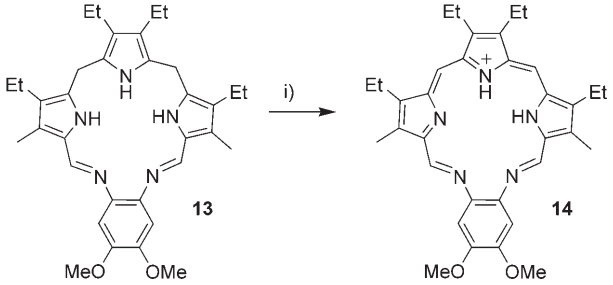

Scheme 5. Synthesis of free base texaphyrin: i) $[Cp_2Fe]PF_6$, 2,6-lutidine, CH_3CN.[22]

Acid–base properties of Schiff base macrocycles of type 4: Macrocycles of type **4** are basic due to the presence of imine groups. The UV/Vis spectra of the macrocycles are sensitive

to protonation. Thus, a photometric titration of **4a** with TFA reveals the formation of a monoprotonated species with a bathochromically shifted UV/Vis spectrum (Figure 2). Only one of the two imine nitrogen atoms is protonated, even in the presence of a fourfold excess of TFA. Accordingly, macrocycles **4a–d** also lose their twofold ^{1}H NMR symmetry in the presence of TFA. For example, for **4a**·TFA, the phenylene signals ($\delta = 7.17$ ppm) split into two doublets of doublets, and a new signal at $\delta = 11.15$ ppm (br s, 1H; protonated imine) is observed. The chromophore in these compounds includes the diamine linker, as can be deduced by the sensitivity of the UV/Vis spectrum toward the particular linker used. For instance, the spectrum of **4d** containing a C_3 aliphatic linker is clearly hypsochromically shifted ($\lambda_{max} = 312$ nm) relative to **4c** ($\lambda_{max} = 342$ nm), which contains an aromatic linker. Bringing two chromophores into conjugation, as in **4e**, causes a 30–40 nm bathochromic shift relative to the monomacrocyclic compound **4a**, whereas a mere linking of the chromophores through a biphenyl linkage (**4f**) causes a redshift of less than 10 nm.

Spectrophotometric titration of the bis-macrocyclic compounds **4e**,**f** with TFA revealed a 2:1 TFA/macrocycle ratio upon protonation but with no discernable isosbestic point. A titration with diacids, such as hexafluoroglutaric or perfluorosuberic acid, confirmed the expected 1:1 diacid/macrocycle ratio upon protonation (see Figures S26 and S27 in the Supporting Information). This raises the question as to whether the diacids would hydrogen bond in an intramolecular fashion, that is, linking both macrocyclic moieties within one molecule, or if extended chain structures would be formed. The UV/Vis spectrum of **4e**,**f** with both diacids is somewhat broadened but otherwise identical to the spectrum observed for the protonation with the monoacid TFA, including the absence of isosbestic points. This may point toward some minor diacid-induced changes in the conformation of the chromophores, or, most likely, the presence of multiple species as a result of nonspecific **4e,f**·2H$^+$-diacid–dianion interactions. If intramolecular hydrogen bonding had predominantly taken place, we would not have expected the two diacids of differing chain lengths to show near-identical results. The short diacid, hexafluoroglutaric acid, was predicted to be incapable of forming hydrogen bonds with both macrocyclic cavities of a single molecule of **4e**,**f**, whereas perfluorosuberic acid was predicted to be able to span both macrocyclic subunits in an intramolecular fashion. A series of ^{19}F and ^{1}H NMR investigations (in [D$_6$]DMSO) also pointed to the presence of multiple species.

Structural variety of 4 and 4·TFA in the solid state: Figure 3 shows the single-crystal X-ray structure of free base **4a**, present as the solvate **4a**·2EtOH. The macrocycle assumes a nonplanar, shallow bowl-shape conformation. The imine functionalities and the two sp^2-carbon-linked pyrrole moieties are each idealized coplanar, and the angle between the mean planes of the pyrrole moieties and the phenylene ring is 41°. The sp^3-carbon-linked pyrazole ring is slanted by about 80° relative to the phenylene plane. Notably, the nitrogen atoms of the pyrazole ring are positioned outside of the macrocycle cavity. This relative orientation of the pyrazole moieties was also predicted by molecular modeling studies to be the prevalent conformation in pyrazole-based polyamine macrocycles.[8b] The pyrazole nitrogen atoms are thus not engaged in intramolecular hydrogen bonding but they give rise to intermolecular hydrogen bonds to two molecules of EtOH, whereby one nitrogen atom acts as hydrogen-bond donor, the other as acceptor. These cocrystallized solvents act as bridges between macrocycles, forming dimers that display their pyrazole nitrogen atoms in a complementary fashion toward each other. One more (disordered) EtOH molecule is found hydrogen bonded in a four-point arrangement to both imine nitrogen atoms and both pyrrole NH protons. This might suggest that the cavity of free base macrocycles of type **4** is well suited to accommodate ROH (and, perhaps, other) guests through its combined hydrogen-bond donor/acceptor arrangement.

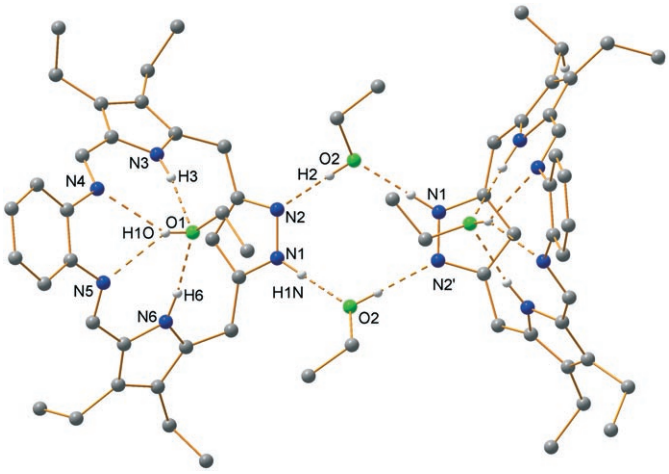

Figure 3. View of the intermolecular hydrogen-bonding interactions of **4a**·2EtOH as observed in the solid state. All hydrogen atoms not involved in hydrogen bonding and the disorder of the C_2H_5 group have been omitted for clarity. Selected interatomic distances [Å] and angles [°]: N3···O1 2.906(2), N3–H3 0.92(3), O1···N4 2.962(2), O1···N5 2.934(2), O1–H1O 0.82(3), N6···O1 2.920(2), N6–H6 0.94(3), N1···O2′ 2.783(2), N1–H1N 0.92(3), O2···N2 2.778(2), O2–H2 0.87(3), N4–C13 1.283(3), N4–C14 1.407(3), N5–C20 1.278(3), N5–C19 1.416(3); N3-H3···O1 172(3), O1-H1O···N4 143(3), O1-H1O···N5 141(3), N6-H6···O1 171(2), N1-H1N···O2′ 179(2), O2-H2···N2 179(3), C13-N4-C14 121.3(2), C20-N5-C19 120.8(2). Symmetry transformation used to generate equivalent atoms (′): $-x$, y, $0.5-z$.

As noted above, macrocycles of type **4** are basic and their trifluoroacetate salts crystallize readily from the crude reaction mixture. This allowed the determination of the solid-state conformational changes that occur upon protonation (Figure 4). The phenylene–imine–pyrrole portion of the protonated macrocycle **4a**·TFA·H$_2$O now takes up a more planar conformation, reducing the angle between the mean planes of the pyrrole moieties and the phenylene ring to 18°. The pyrazole moiety assumes essentially the same conformation as in the free base form, albeit with the ring only slanted by about 65° relative to the phenylene plane. The protonation-induced planarization—with, presumably, con-

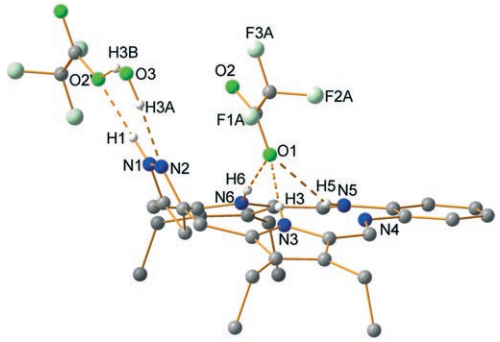

Figure 4. View of the intermolecular hydrogen-bonding interactions of **4a**·TFA·H_2O as observed in the solid state. All hydrogen atoms not involved in hydrogen bonding and the disorder of the CF_3 group have been omitted for clarity. Selected interatomic distances [Å] and angles [°]: N3···O1 2.931(3), N3–H3 0.87(3), N5···O1 3.242(3), N5–H5 0.90(3), N6···O1 2.824(3), N6–H6 0.96(4), N1···O2′ 2.838(3), N1–H1 0.94(4), O3···N2 2.912(3), O3···O2′ 2.749(3), O3–H3A 0.95(5), O3–H3B 1.01(5), N4–C13 1.290(3), N4–C14 1.412(3), N5–C20 1.319(3), N5–C19 1.416(3); N3-H3···O1 170(3), N5-H5···O1 145(2), N6-H6···O1 166(3), N1-H1···O2′ 164(3), O3-H3A···N2 164(4), O3-H3B···O2′ 161(4), C13-N4-C14 121.6(2), C20-N5-C19 127.8(2). Symmetry transformation used to generate equivalent atoms (′): $1-x$, $2-y$, $2-z$.

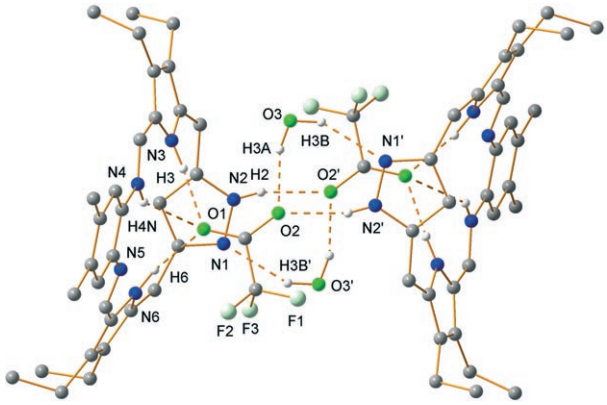

Figure 5. View of the intermolecular hydrogen-bonding interactions of **4b**·TFA·H_2O as observed in the solid state. In the interest of clarity all hydrogen atoms not involved in hydrogen bonding have been omitted. Selected interatomic distances [Å] and angles [°]: N2···O2′ 2.878(4), O3···O2 2.752(4), O3···N1′ 3.056(4); N2-H2···O2′ 167(5), O3-H3A···O2 155(6), O3-H3B···N1′ 154(5). Symmetry transformation used to generate equivalent atoms (′): $1-x$, $1-y$, $2-z$.

comitant rigidification—of the chromophore is also seen in the sharpened and increased UV/Vis absorption of the protonated macrocycles (Figure 2).

These changes brought about by protonation of a single imine moiety appear to be general in this compound class because they are also observed in the solid-state structures of **4b**·TFA·H_2O (Figure 5) and **4c**·TFA·H_2O (Figure 6). The conformational changes are concomitant with a change in the intramolecular hydrogen-bond patterns. The protonated imine functionality switched from being a hydrogen-bond acceptor (in free base **4a**) to a hydrogen-bond donor that is bonded to, in all cases, a molecule of trifluoroacetate that sits above the mean plane of the macrocycle and that is also hydrogen bonded to other sites of the macrocycle. These trifluoroacetate molecules, together with the water molecules, act as hydrogen-bonding bridges to the pyrazole NH functionality of a second molecule of protonated **4**. However, significant differences between the final outcome of these hydrogen bonds in the structures of **4a**·TFA·H_2O/**4b**·TFA·H_2O and **4c**·TFA·H_2O are observed. Whereas a pair of trifluoroacetate molecules and H_2O molecules link two protonated macrocycles of **4a** and **4b** to form a dimer, an infinite chain is formed by **4c**·TFA·H_2O.

The propensity of the protonated macrocycles to form hydrogen-bonded aggregates was also detected in their single and tandem ESI+ mass spectra, which generally show peaks with m/z values that correspond to a number of mono- and dicationic dimer structures held together by one or two protons and/or trifluoroacetate anions, such as $[\mathbf{4a}\cdot H]^+$ (m/z 467), $[\mathbf{4a}\cdot H\cdot\mathbf{4a}]^+$ (m/z 933), or $[\mathbf{4a}\cdot H\cdot TFA\cdot\mathbf{4a}]^+$ (m/z 1046). Furthermore, the signals for the pyrazole and pyrrole NH protons are substantially broadened in the ^1H NMR spectrum (in $CDCl_3$) of the protonated macrocycles, which is also indicative of their involvement in intra- or intermolecular hydrogen bonds.

The number of well-defined and switchable hydrogen-bond donor and acceptor opportunities at the in- and outside of the macrocycle, combined with a chromophore that is sensitive to changes in the hydrogen-bond pattern and protonation state, makes macrocycles of type **4** unique and suggests that the free base and protonated compounds could be used in molecular-recognition systems.

Testing the anion-recognition abilities of 4a and 4a·H$^+$: We tested whether anion-specific spectroscopic properties of **4a**·H^+ can be discerned. The results of a UV/Vis titration study of **4a** with a variety of organic and inorganic acids are shown in Figure 7 (titration profiles for the systems **4a**/PFP and **4a**/DMP can be found in Figures S24 and S25 in the Supporting Information). To our disappointment, no anion-specific features in the UV/Vis spectra of the **4a**·H^+·acid anion were detected. We surmise that (nonspecific) electrostatic cation–anion interactions override, if at all present, any specific anion-recognition effects.

We therefore tested the neutral macrocycles toward anion-recognition effects. That the neutral compound **4a** is, in fact, capable of distinct interactions with anions is shown by an NMR titration of **4a** with tetra-*n*-butylammonium fluoride (TBAF) in [D_6]DMSO. The pyrazole CH region of the ^1H NMR spectrum of **4a** is shown in Figure 8. Upon addition of fluoride, a $\delta \approx 0.6$ ppm upfield shift of the CH^{pz} signal is observed. The computed binding constant for this interaction is about $15\,M^{-1}$ and therefore much weaker than many other pyrrole-based systems.[2] The shift of the pyrazole CH group may indicate the hydrogen bonding of fluoride to the pyrazole NH functionality on the outside of the macrocycle (cf. to Figure 3), or may be the result of fluoride binding to one, or both NH functionalities of the pyrroles at the inside of the macrocycle. The proximity of the CH^{pz} hy-

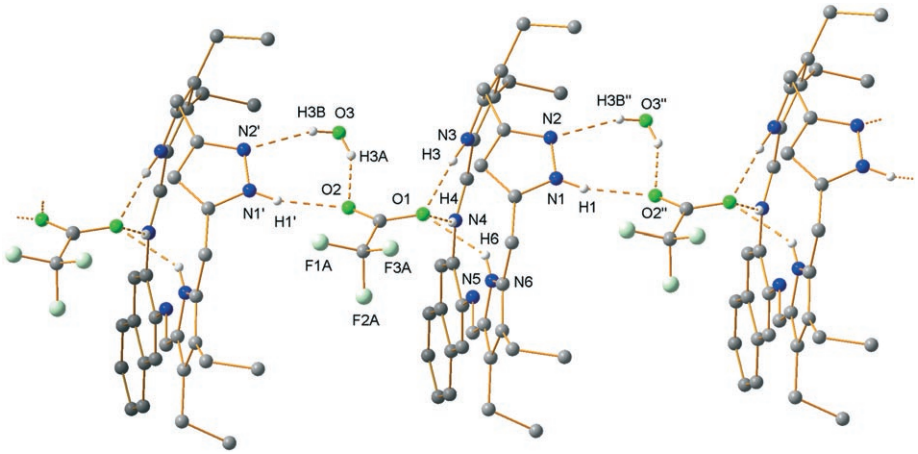

Figure 6. View of the intermolecular hydrogen-bonding interactions of **4c**·TFA·H_2O as observed in the solid state. In the interest of clarity all hydrogen atoms not involved in hydrogen bonding have been omitted. Selected interatomic distances [Å] and angles [°]: N1···O2″ 2.871(4), O3···O2 2.840(5), O3···N2′ 3.002(5); N1-H1···O2″ 156(5), O3-H3A···O2 152(4), O3-H3A···N2′ 162(5). Symmetry transformations used to generate equivalent atoms (′): $-1+x, y, z$; (″): $1+x, y, z$.

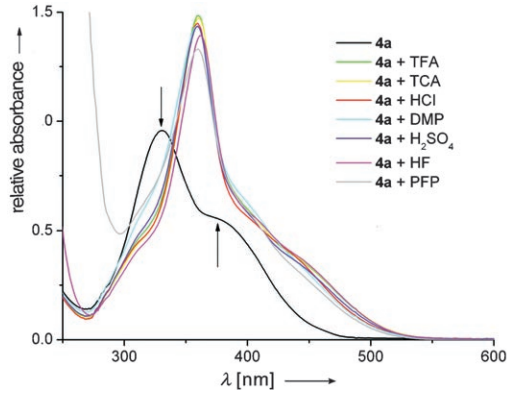

Figure 7. UV/Vis spectra of **4a** in THF in the presence of different acids (TFA: trifluoroacetic acid; TCA: trichloroacetic acid; DMP: dimethylphosphate; PFP: pentafluorophenol).

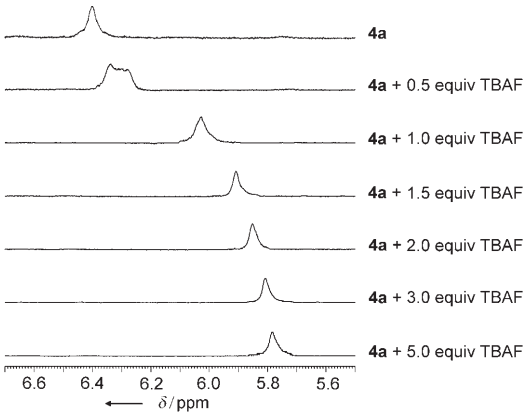

Figure 8. ^{1}H NMR spectrum of the titration of macrocycle **4a** (6.77×10^{-2} M in [D_6]DMSO) with a solution of $n$$Bu_4$NF (1.02 M).

drogen atom pointing toward the center of the macrocycle and the bound fluoride would then account for the observed shift. However, given that the only signal affected by the addition of fluoride is that of the CH^{pz} hydrogen atom, binding to the pyrazole group is most likely. No significant changes in the UV/Vis spectrum of **4a** are detected in the presence of F^-, further supporting NH^{pz} binding at this position that is not part of the chromophore. Variable temperature ^{19}F NMR experiments proved to be of no value to discern the binding mode. Fluoride binding to pyrrole nitrogen atoms is well known and much exploited.[2] Evidently, however, in **4a** fluoride binding to a pyrazole NH group is preferred, further encouraging us to pursue the design of pyrrole–pyrazole conjugates that are capable of projecting both types of hydrogen-bond donor toward the inside of the molecule.

Conclusion

In summary, the linear pyrrole–pyrazole hybrid **5c** and its precursor **6** provide new and useful building blocks for the construction of novel macrocycles containing pyrazole and pyrrole moieties, with the family of mono- and bicyclic Schiff base compounds **4** presented here as a first example. In that vein, we are currently exploring the cyclocondensation of **5c** with **6** to form the pyrazole analogues of hexaphyrin or Furuta's 'doubly N-confused hexaphyrin'.[24] The combination of the presence of a chromophore, defined conformation, and multiple hydrogen-bond sites at the in- and outside of the macrocycle suggest the use of **4** in molecular-recognition systems. Some indications for fluoride binding of the neutral macrocycles were found, though binding affinity and selectivity were modest, at best. Nevertheless, the structures and ease of synthesis of these novel systems, in combination with their unique pattern of hydrogen-bonding donor and acceptor sites, warrant their further investigation. We are currently investigating the metal coordination properties of type **4** macrocycles.

Experimental Section

General: NMR spectra were measured by using Bruker Avance spectrometers and are reported on the δ scale. ^{19}F NMR spectra were referenced against C_6F_6. Where necessary, assignment of the NMR signals was derived from 2D spectra; abbreviations used in the assignments: py = pyr-

role, pz = pyrazole. Mass spectra were recorded by using Finnigan MAT 8200 (EI), Finnigan MAT LCQ (ESI), or Finnigan MAT 95 (FAB) mass spectrometers and the high-resolution mass spectra were recorded by using a Bruker APEX IV 7 T Fourier transform ion cyclotron resonance (FTICR) machine. IR data were collected with a Digilab Excalibur spectrometer. UV/Vis spectra were recorded by using an Analytik Jena Specord S 100 spectrometer in a 1 cm pathway cuvette. Melting points were determined by using a Büchi melting point B-540 apparatus or a Stanford Research Systems Scientific Instruments GmbH Optimelt MPA 100 and are uncorrected. Elemental analyses were measured by the Analytical Laboratory of the Institut für Anorganische Chemie der Universität Göttingen by using a Heraeus CHN-O-RAPID instrument. Solvents were dried (P_4O_{10} for CH_2Cl_2, Mg for MeOH, and CaH_2 for DMF) and distilled prior to use. 3,5-Bis(chloromethyl)- (**8a**)[16,17] and 3,5-bis(bromomethyl)-1-(tetrahydropyran-2-yl)pyrazole hydrochloride (**8b**),[15] 3,5-bis(chloromethyl)-1*H*-pyrazole (**11**),[13] and 3,4-diethylpyrrole (**7c**)[25] were prepared according to literature procedures. All other reagents were commercially available and were used as received. Column chromatography was performed on aluminum oxide (Macherey-Nagel AG, basic, Brockmann Activity I), unless otherwise indicated. Analytic thin-layer chromatography (TLC) was carried out using aluminum oxide (layer thickness 0.2 mm) aluminum-backed TLC cards with fluorescent indicator (254 nm) purchased from Fluka.

3-Chloromethyl-5-(1*H*-pyrrol-2-ylmethyl)-1-(tetrahydropyran-2-yl)pyrazole (9) and 3,5-bis(1*H*-pyrrol-2-ylmethyl)-1-(tetrahydropyran-2-yl)pyrazole (10): Pyrrole (**7a**) (2.40 mL, 34.0 mmol) was dissolved, under anhydrous conditions (N_2), in dry THF (30 mL). The reaction mixture was cooled in an acetone/dry ice bath to −30 °C and *n*BuLi (1.6 M in hexane, 21.3 mL, 34.0 mmol) was added carefully in portions. After stirring for 1.5 h, compound **8a** (1.0 equiv, 2.13 g, 8.53 mmol) dissolved in dry THF (30 mL) was added dropwise. The reaction was stirred for 5 h at −40 °C. Subsequently, the reaction was allowed to warm to room temperature overnight. A saturated aqueous NH_4Cl solution (100 mL) was added and the mixture was extracted with CH_2Cl_2 (2×100 mL). The combined organic layers were dried over $MgSO_4$, filtered, and the solvent was removed by using rotary evaporation to yield a brown oil that was purified by means of column chromatography (aluminum oxide, basic, Brockmann activity I, ethyl acetate/light petroleum 1:2). After the removal of the solvent, product **10** was obtained as a hygroscopic light brown solid. This should be stored at low temperature and under an N_2 atmosphere. (Second fraction eluting from the column was **9** (0.068 mg, 29 %); third fraction was **10** (0.442 g, 17 %)). Compound **9**: R_f = 0.62 (aluminum oxide, ethyl acetate/petroleum ether 1:2); ^{1}H NMR (300 MHz, $CDCl_3$, 301 K): δ = 1.52–1.74 (m, 3H; CH_2^{THP}), 1.88–1.92 (dd, ^3J(H,H) = 13.3, 3.6 Hz, 1H; CH_2^{THP}), 2.02–2.09 (m, 1H; CH_2^{THP}), 2.36–2.47 (m, 1H; CH_2^{THP}), 3.62 (t, J^3(H,H) = 11.4 Hz, 1H; CH_2^{THP}), 3.98–4.06 (m, 3H; CH_2-py, 2H; CH_2^{THP}, 1H), 4.50–4.56 (m, 2H; CH_2-Cl), 5.27 (dd, J^3-(H,H) = 7.5 Hz, J^4(H,H) = 2.6 Hz, 1H; C$H^{THP\text{-}pz}$), 5.99–6.02 (m, 1H; C$H^{py(\beta)}$), 6.09–6.11 (q, J^3(H,H) = 5.8, J^4(H,H) = 2.7 Hz, 1H; CH^{py}), 6.13 (s, 1H; CH^{pz}), 6.63–6.65 (m, J^3(H,H) = 2.6 Hz, 1H; C$H^{py(\alpha)}$), 8.42 ppm (s, 1H; N*H*); ^{13}C NMR (125 MHz, $CDCl_3$, 298 K): δ = 22.6 (CH_2^{THP}), 24.3 (CH_2), 28.8 (CH_2^{THP}), 29.4 (CH_2^{THP}), 39.2 (Cl-CH_2), 67.9 (CH_2^{THP}), 84.7 (N-CH^{THP}), 106.2 (CH^{pz}), 106.4 ($CH^{py(\beta)}$), 108.3 (CH^{py}), 117.6 ($CH^{py(\alpha)}$), 127.1 ($C^{q,py}$), 142.6 (N=$C^{q,pz}$), 148.6 ppm (N=$C^{q,pz}$); IR (KBr): $\tilde{\nu}$ = 3347 (m), 2945 (s), 2852 (s), 1551 (w), 1466 (m), 1254 (s), 1083 (s), 1042 (vs), 1005 (s), 799 (s), 728 cm^{-1} (s); MS (EI): *m*/*z* (%): 279 (28) $[M]^+$, 244 (8) $[M-Cl]^+$, 195 (100) $[M-THP+H]^+$, 160 (17) $[M-THP-Cl]^+$, 85 (66) $[DHP-H]^+$; elemental analysis calcd (%) for $C_{14}H_{18}N_3OCl$: C 60.10, H 6.49, N 15.02, O 5.72, Cl 12.67; found: C 60.33, H 6.91, N 13.60. Compound **10**: R_f = 0.39 (aluminum oxide, ethyl acetate/petroleum ether 1:2); ^{1}H NMR (300 MHz, $CDCl_3$, 301 K): δ = 1.55–1.78 (m, 3H; CH_2^{THP}), 1.90 (m, 1H; CH-CH_2^{THP}), 2.10 (m, 1H; CH_2^{THP}), 2.41–2.52 (m, 1H; CH-CH_2^{THP}), 3.57–3.68 (td, ^3J(H,H) = 11.4 Hz, ^4J(H,H) = 2.2 Hz, 1H; CH_2^{THP}), 3.87–3.94 (dd, ^3J(H,H) = 16.4 Hz, 2H; CH_2), 3.92–4.04 (dd, ^3J(H,H) = 16.5 Hz, 2H; CH_2), 4.03–4.12 (m, 1H; CH_2^{THP}-O), 5.24 (dd, ^3J(H,H) = 10.2/2.5 Hz, 1H; -O-CH^{THP}), 5.86 (s, 1H; CH^{pz}), 5.96–5.98 (m, 2H; $CH^{py(\beta)}$), 6.06–6.10 (q, ^3J(H,H) = 8.6 Hz, ^4J(H,H) = 2.8 Hz, 2H; CH^{py}), 6.64 (m, 2H; $CH^{py(\alpha)}$), 8.53 ppm (s, 1H; NH); ^{13}C NMR (125 MHz, $CDCl_3$, 301 K): δ = 22.9 (CH_2^{THP}), 24.2 (CH_2), 26.9 (CH_2), 24.8 (CH_2^{THP}), 29.7 (CH_2^{THP}), 68.1 (CH_2^{THP}-O), 84.5 (CH^{THP}), 105.7 (CH^{pz}), 106.1 ($CH^{(\beta)}$), 106.2 ($CH^{(\beta)}$), 108.1 (CH^{py}), 108.2 (CH^{py}), 116.8 ($CH^{py(\alpha)}$), 117.5 ($CH^{py(\alpha)}$), 127.4 ($C^{q,py}$), 129.2 ($C^{q,py}$), 141.8 ($C^{q,pz}$), 150.6 ppm ($C^{q,pz}$); MS (EI): *m*/*z* (%): 310 (35) $[M]^+$, 226 (100) $[M-THP+H]^+$, 159 (75) $[M-THP-py]^+$, 85 (99) $[DHP+H]^+$.

3,5-Bis(1*H*-pyrrol-2-ylmethyl)-1*H*-pyrazole (6a): A solution of pyrrole (**7a**) (3.4 mL, 48.8 mmol) in CH_2Cl_2 (dry, 40 mL) was cooled in an acetone/dry ice bath to −78 °C under an N_2 atmosphere and *n*BuLi (1.6 M in hexane, 30.5 mL, 48.8 mmol) was added carefully in portions. After stirring for 1 h, compound **11** (1.0 equiv, 2.50 g, 12.5 mmol) dissolved in dry CH_2Cl_2 (20 mL) was added dropwise. The reaction mixture was stirred for 4 h at −78 °C and was then allowed to warm to room temperature overnight. A saturated aqueous NH_4Cl solution (100 mL) was added and the mixture was extracted with CH_2Cl_2 (3×100 mL). The combined organic layers were dried over Mg_2SO_4, filtered, and the solvent was removed by using rotary evaporation to yield a brown oil that was purified by means of column chromatography (aluminum oxide, basic, Brockmann activity I, diethyl ether/petroleum ether 7:1). After removal of the solvent, compound **6a** was obtained as a hygroscopic white solid (567 mg, 21 %). The product is susceptible to fast decomposition at room temperature in air and is best kept in the freezer under N_2. R_f = 0.20 (aluminum oxide, diethyl ether/light petroleum 7:1); ^{1}H NMR (300 MHz, $CDCl_3$, 300 K): δ = 3.85 (s, 4H; CH_2), 5.88 (s, 1H; CH^{pz}), 5.96–5.97 (m, 2H; CH^{py}), 6.05–6.09 (m, 2H; CH^{py}), 6.55–6.57 (m, 2H; CH^{py}), 8.61 ppm (s, 2H; NH); ^{13}C NMR (125.76 MHz, $CDCl_3$, 300 K): δ = 25.6 (CH_2), 103.8 ($CH^{py(\beta)}$), 106.6 (CH^{pz}), 108.4 (CH^{py}), 117.6 ($CH^{py(\alpha)}$), 128.3 (C^q), 147.0 ppm ($C^{q,pz}$); MS (EI): *m*/*z* (%): 226 (100) $[M]^+$, 160 (22) $[M-py]^+$, 152 (54) $[M-CH_2py]^+$, 80 (20) $[pz-CH_2]^+$, 67 (49) $[py+H]^+$.

3,5-Bis(5-methyl-1*H*-pyrrol-2-ylmethyl)-1*H*-pyrazole (6b): Prepared from 2-methylpyrrole **7b** (2.60 g, 29.3 mmol) and **11** (1.0 equiv, 1.20 g, 7.30 mmol) as described for **6a** and purified by means of column chromatography (aluminum oxide, CH_2Cl_2/MeOH/Et_3N 10:1:0.001). The second, main fraction was collected, providing **6b** as a light ochre solid (1.63 g, 88 %). R_f = 0.54 (aluminum oxide, CH_2Cl_2/MeOH 10:1); m.p. 73–77 °C; ^{1}H NMR (400 MHz, $CDCl_3$, 298 K): δ = 2.18 (s, 6H; CH_3), 3.88 (s, 4H; CH_2), 5.77 (m, 2H; CH^{py}), 5.89 (m, 2H; CH^{py}), 5.95 (s, 1H; CH^{pz}), 8.20 ppm (brs; NH); ^{13}C NMR (100.63 MHz, $CDCl_3$, 298 K): δ = 13.0 (CH_3), 37.7 (CH_2), 38.2 (CH_2), 103.5 (CH^{py}), 105.9 (CH^{pz}), 106.3 (CH^{py}), 127.5 ppm ($C^{q,py}$); IR (KBr): $\tilde{\nu}$ = 3348 (s), 3228 (s), 2916 (s), 1666 (w), 1574 (w), 1425 (m), 1303 (w), 1142 (w), 1001 (w), 769 cm^{-1} (s); MS (EI): *m*/*z* (%): 254 (100) $[M]^+$, 173 (44) $[M-(C_5H_7N)]^+$, 94 (20) $[CH_2pyCH_3]^+$, 80 (18) $[py-CH_3]^+$; elemental analysis calcd (%) for $C_{15}H_{18}N_4$: C 70.84, H 7.13, N 22.03; found: C 70.34, H 7.37, N 20.89.

3,5-Bis(3,4-diethyl-1*H*-pyrrol-2-ylmethyl)-1*H*-pyrazole (6c): Prepared from 3,4-diethylpyrrole (**7c**) (3.5 g, 28.4 mmol) dissolved in dry CH_2Cl_2 (200 mL) and 3,5-bis(chloromethyl)-1*H*-pyrazole (**11**) (1.0 equiv, 1.33 g, 8.10 mmol) dissolved in dry CH_2Cl_2 (50 mL), as described for **6a**, and purified by means of column chromatography (aluminum oxide, CH_2Cl_2/MeOH 45:1). After the removal of the solvent, compound **6c** was obtained as a hygroscopic, low-melting light brown solid (2.49 g, 91 %). The product is susceptible to slow decomposition at room temperature in air and is best kept in the freezer under N_2. R_f = 0.50 (aluminum oxide, CH_2Cl_2/MeOH 1:20); m.p. 36–45 °C; ^{1}H NMR (500 MHz, $CDCl_3$, 301 K): δ = 1.11–1.14 (t, ^3J(H,H) = 7.5 Hz, 6H; CH_3), 1.21–1.24 (t, ^3J(H,H) = 7.51 Hz, 6H; CH_3), 2.45–2.51 (m, ^3J(H,H) = 7.5 Hz, 8H; CH_2CH$_3$), 3.83 (s, 4H; py-CH_2-pz), 5.88 (s, 1H; CH^{pz}), 6.33 (s, 1H; CH^{py}), 6.34 (s, 1H; CH^{py}), 8.19 (brs, 2H; NH), 8.69–10.19 ppm (brs; NH); ^{13}C NMR (126 MHz, $CDCl_3$, 301 K): δ = 14.6 (CH_3), 16.1 (CH_3), 17.4 (CH_2), 18.5 (CH_2), 23.8 (py-CH_2-pz), 103.5 (CH^{pz}), 112.8 (CH^{py}), 120.3 (C^q), 123.8 (C^q), 124.8 (C^q), 147.1 ppm (C^{pz}); IR (KBr): $\tilde{\nu}$ = 3356 (s), 2926 (m), 1674 (m), 1558 (m), 1443 (s), 1298 (w), 1083 (w), 1002 (w), 779 (m), 532 cm^{-1} (m); MS (EI): *m*/*z* (%): 338 (62) $[M]^+$, 323 (10) $[M-CH_3]^+$, 309 (7) $[M-C_2H_5]^+$, 217 (20) $[M-C_8H_{11}N]^+$, 200 (22) $[M-C_9H_{16}N]^+$, 186 (5) $[M-C_{10}H_{18}N]^+$, 154 (12) $[C_9H_4N_3]^+$, 122 (100) $[C_8H_{12}N]^+$; HRMS (ESI+, methanol/water): *m*/*z* calcd for $C_{21}H_{31}N_4$: 339.25432 $[M+H]^+$; found: 339.25433 $[M+H]^+$; elemental analysis calcd (%) for $C_{21}H_{30}N_4 \cdot 0.25\,H_2O$: C 73.52, H 8.97, N 16.34; found: C 73.59, H 8.67, N 16.45.

3,5-Bis(3,4-diethyl-5-formyl-1*H*-pyrrol-2-ylmethyl)-1*H*-pyrazole (5c): A procedure for the diformylation of dipyrromethanes was adopted from the literature:[26] Under an N_2 atmosphere, benzoyl chloride (0.76 mL, 6.7 mmol, 8.0 equiv) was added to an ice-cooled solution of compound **6c** (282 mg, 0.83 mmol) in dry DMF (608 mg, 8.33 mmol, 10 equiv). The reaction mixture was stirred at 0 °C for 2 h, followed by an additional 4 h at RT. (For larger scale preparations we recommend stirring the reaction mixture for several hours longer.) The dark brown mixture was cooled back to 0 °C and quenched by addition of a wet, ethanolic Na_2CO_3 solution (1.0 g Na_2CO_3 dissolved in 80 mL 1:1 H_2O/EtOH). The solution was extracted with CH_2Cl_2 (3×100 mL), the combined organic phase was dried over Na_2SO_4, and evaporated to dryness in vacuo. The resulting black oil was purified by means of column chromatography (aluminum oxide, basic, CH_2Cl_2/MeOH 20:1). The third, main fraction was collected and the solvent was evaporated under vacuum to afford **5c** as a light brown solid. Subsequent recrystallization from EtOH gave **5c** as a light ochre solid (288 mg, 88 %; the yields of multi-gram preparations were reduced to 40–70 %). R_f = 0.44 (aluminum oxide, CH_2Cl_2/MeOH 15:1); m.p. 191–195 °C; ^{1}H NMR (500 MHz, [D$_6$]DMSO, 301 K): δ = 0.89–0.92 (t, ^3J(H,H) = 7.5 Hz, 6H; CH_3), 1.09–1.12 (t, ^3J(H,H) = 7.5 Hz, 6H; CH_3), 2.29–2.33 (q, ^3J(H,H) = 7.5 Hz, 4H; CH_2CH$_3$), 2.60–2.65 (q, ^3J(H,H) = 7.5 Hz, 4H; CH_2CH$_3$), 3.80 (s, 4H; py-CH$_2$-pz), 5.74 (s, 1H; CH^{pz}), 9.45 (s, 2H; CHO), 11.40 (brs; NH), 12.28 ppm (brs; NH); ^{13}C NMR (126 MHz, [D$_6$]DMSO, 301 K): δ = 15.8 (CH_3), 16.2 (*C*H$_2$CH$_3$), 16.6 (*C*H$_2$CH$_3$), 17.4 (CH_3), 23.4 (br; py-*C*H$_2$-pz), 102.7 (CH^{pz}), 122.9 (C^q), 127.0 (*C*^{py}CHO), 135.5(C^q), 136.4 (C^q), 144.6 (br; C^q), 176.3 ppm (CHO); IR (KBr): $\tilde{\nu}$ = 3243 (s), 2929 (m), 1608 (vs), 1448 (m), 1350 (m), 1280 (w), 1134 (w), 1010 (m), 856 (w), 772 cm^{-1} (s); MS (EI): *m*/*z* (%): 394 (100) [*M*]$^+$, 365 (63) [*M*−C$_2$H$_5$]$^+$, 351 (5) [*M*−C$_3$H$_7$]$^+$, 337 (13) [*M*−2C$_2$H$_5$+H]$^+$, 323 (5) [*M*−2C$_2$H$_5$−CH$_3$+2H]$^+$, 243 (28) [*M*−C$_9$H$_{12}$NO]$^+$, 228 (16) [C$_{13}$H$_{16}$N$_4$]$^+$, 214 (18) [C$_{12}$H$_{14}$N$_4$]$^+$, 200 (12) [C$_{11}$H$_{12}$N$_4$]$^+$, 150 (30) [C$_9$H$_{12}$NO]$^+$, 122 (50) [C$_8$H$_{12}$N]$^+$, 94 (7) [C$_5$N$_2$H$_6$]$^+$; HRMS (ESI+, MeOH/H_2O): *m*/*z* calcd for $C_{23}H_{31}N_4O_2$: 395.24415 [*M*+H]$^+$; found: 395.24413 [*M*+H]$^+$; elemental analysis calcd (%) for $C_{23}H_{30}N_4O_2$·0.5 H_2O: C 68.46, H 7.74, N 13.88; found: C 68.44, H 7.74, N 14.29.

General procedure for the preparation of free base Schiff base macrocycles of type 4: Dialdehyde **5c** (200 mg, 0.51 mmol) was dissolved under N_2 in dry MeOH (250 mL) at 50 °C. The appropriate diamine (0.51 mmol, 1.0 equiv) dissolved in dry MeOH (10 mL) was added dropwise to the stirred solution. After 15 min, TFA (1.54 mL, 20.0 mmol, 40 equiv) was added in small portions and the reaction mixture was heated to reflux under N_2 for 20 h. After this time, the solvent was removed by using rotary evaporation and the resulting (red to brown) residue was purified by means of column chromatography over aluminum oxide.

General procedure for the preparation of Schiff base macrocycle salts of type 4·TFA: The same preparation as described for **4**, however, the chromatographic step over aluminum oxide was replaced by a recrystallization of the crude protonated material. Thus, after cooling the reaction mixture to ambient temperature, the solvent was removed by using the rotary evaporator and the resulting red-to-brown solid was purified by recrystallization.

Schiff base macrocycle 4a: Prepared according to the general procedure for **4** using dialdehyde **5c** (200 mg, 0.51 mmol) and 1,2-diaminobenzene (54.0 mg, 0.51 mmol). Column chromatography (aluminum oxide, basic, Brockmann activity I, CH_2Cl_2/MeOH 30:1) provides **4a** as a yellow-orange solid (213 mg, 90 %, 0.51 mmolar reaction scale). R_f = 0.79 (aluminum oxide, CH_2Cl_2/MeOH 30:1); m.p. 241–244 °C; ^{1}H NMR (500 MHz, $CDCl_3$, 301 K): δ = 1.01–1.04 (t, ^3J(H,H) = 7.5 Hz, 6H; CH_3), 1.16–1.19 (t, ^3J(H,H) = 7.5 Hz, 6H; CH_3), 2.30–2.35 (m, 4H; CH_2CH$_3$), 2.53–2.57 (q, ^3J(H,H) = 7.4 Hz, 4H; CH_2CH$_3$), 3.88 (s, 4H; py-CH$_2$-pz), 5.67 (s, 1H; CH^{pz}), 7.17 (s, 4H; CH^{Ph}), 8.16 (s, 2H; HC=N), 10.50 ppm (brs; NH); ^{13}C NMR (126 MHz, $CDCl_3$, 301 K): δ = 16.0 (CH_3), 17.0 (*C*H$_2$CH$_3$), 17.3 (*C*H$_2$CH$_3$), 17.4 (CH_3), 24.0 (br; py-*C*H$_2$-pz), 103.9 (CH^{pz}), 117.2 (br; C^{Ph}), 122.6 (C^{tert}), 125.7 (C^{Ph}), 132.5 (br; C^{tert}), 146.1 ppm (br; HC=N); IR (KBr): $\tilde{\nu}$ = 3428 (m), 3268 (w), 3061 (w), 2961 (m), 2926 (w), 2868 (w), 1614 (vs), 1569 (s), 1443 (s), 1383 (w), 1335 (w), 1264 (m), 1210 (m), 1101 (w), 1057 (w), 1010 (w), 963 (w), 894 (w), 807 (w), 745 cm^{-1} (w); UV/Vis ($CHCl_3$/0.01 % Et_3N): λ_{max} (ε) = 331 (2.37×10^4 L mol^{-1} cm^{-1}), 362 nm (sh); MS (ESI in MeOH): *m*/*z* (%): 467 (100) [*M*+H]$^+$; MS (FAB in 4-NBA): *m*/*z* (%): 467 (100) [*M*+H]$^+$; HRMS (ESI+, MeOH/H_2O): *m*/*z* calcd for $C_{29}H_{35}N_6$: 467.29177 [*M*+H]$^+$; found: 467.29177 [*M*+H]$^+$; elemental analysis calcd (%) for $C_{29}H_{34}N_6$·1.5 CH_3OH (514.7): C 71.18, H 7.83, N 16.33; found: C 71.19, H 7.49, N 16.04.

Schiff base macrocycle 4a·TFA: Prepared according to the general procedure for **4**·TFA. Isolation and purification by crystallization in MeOH/CH_2Cl_2 at 5 °C over one day. M.p. 222–235 °C; ^{1}H NMR (500 MHz, $CDCl_3$, 301 K): δ = 1.13–1.16 (t, ^3J(H,H) = 7.5 Hz, 6H; CH_3), 1.17–1.20 (t, ^3J(H,H) = 7.5 Hz, 6H; CH_3), 2.50–2.54 (m, 4H; CH_2CH$_3$, [D$_6$]DMSO), 2.73–2.78 (q, ^3J(H,H) = 7.5 Hz, 4H; CH_2CH$_3$), 3.42 (br; NH), 4.13 (s, 4H; py-CH$_2$-pz), 6.21 (s, 1H; CH^{pz}), 7.30–7.34 (dd, ^3J(H,H) = 3.3 Hz, 2H; CH^{Ph}), 7.80–7.82 (dd, ^3J(H,H) = 3.3 Hz, 2H; CH^{Ph}), 8.62 (s, 2H; 2HC=N), 11.15 ppm (brs; NH); ^{13}C NMR (126 MHz, [D$_6$]DMSO, 301 K): δ = 15.1 (CH_3), 16.2 (*C*H$_2$CH$_3$), 16.6 (*C*H$_2$CH$_3$), 17.0 (CH_3), 24.2 (br; py-*C*H$_2$-pz), 104.4 (CH^{pz}), 116.7 (CH^{Ph}), 123.1 (C^q), 125.2 (C^q), 126.6 (CH^{Ph}), 136.0 (C^q), 141.1 (br; C^q), 142.3 (br; HC=N), 157.5 ppm (C^{q,pz}); ^{19}F NMR (188 MHz, [D$_6$]DMSO, 301 K): 89.0 ppm (s; C*F*$_3$COO); IR (KBr): $\tilde{\nu}$ = 3430 (m), 3210 (w), 3178 (w), 2957 (m), 2947 (w), 1640 (vs), 1570 (s), 1552 (w), 1435 (w), 1304 (w), 1190 (m), 1180 (m), 1010 (w), 958 (w), 801 (m), 756 cm^{-1} (w); UV/Vis ($CHCl_3$/TFA): λ_{max} (ε) = 361 (3.58×10^4 L mol^{-1} cm^{-1}), 423 nm (sh); MS (ESI in MeOH): *m*/*z* (%): 467 (58) [*M*+H]$^+$, 933 (78) [2*M*+H]$^+$, 1047 (100) [2*M*+CF$_3$COOH]$^+$.

Schiff base macrocycle 4b: Prepared as a red solid (102 mg, 90 %) according to the general procedure for **4** from **5c** (90 mg, 0.23 mmol) and 4,5-dimethyl-1,2-phenylendiamine (**12b**) (31.0 mg, 0.23 mmol), followed by column chromatography (Brockmann activity I, CH_2Cl_2/MeOH 15:1). R_f = 0.45 (aluminum oxide, MeOH/CH_2Cl_2 1:30); m.p. 216–218 °C; ^{1}H NMR (300 MHz, $CDCl_3$, 298 K): δ = 1.00–1.05 (t, ^3J(H,H) = 7.5 Hz, 6H; CH_3), 1.13–1.18 (t, ^3J(H,H) = 7.5 Hz, 6H; CH_3), 2.27 (s, 6H; 2CH$_3^{Ph}$), 2.31–2.38 (q, ^3J(H,H) = 7.5 Hz, 4H; CH_2CH$_3$), 2.51–2.58 (q, ^3J(H,H) = 7.5 Hz, 4H; CH_2CH$_3$), 3.88 (s, 4H; CH_2), 5.75 (brs, 1H; CH^{pz}), 6.94 (s, 2H; CH^{Ph}), 8.07 ppm (s, 2H; HC=N); NH signal not found; UV/Vis (MeCN/0.01 % Et_3N): λ_{max} (ε) = 334 (2.06×10^4 L mol^{-1} cm^{-1}), 388 nm (sh); MS (ESI in MeCN/CH_2Cl_2): *m*/*z* (%): 495 (100) [*M*+H]$^+$, 989 (65) [2*M*+H]$^+$.

Schiff base macrocycle 4b·TFA: Prepared according to the general procedure for **4**·TFA. Purified by crystallization in MeOH/Et_2O for one day at 5 °C (102 mg, 90 %, 0.23 mmolar scale). R_f = 0.45 (aluminum oxide, MeOH/CH_2Cl_2 1:30); m.p. 216–218 °C; ^{1}H NMR (500 MHz, [D$_6$]DMSO, 301 K): δ = 1.12–1.15 (t, ^3J(H,H) = 7.5 Hz, 6H; CH_3), 1.16–1.19 (t, ^3J(H,H) = 7.5 Hz, 6H; CH_3), 2.29 (s, 6H; 2CH$_3^{Ar}$), 2.49–2.53 (q, ^3J(H,H) = 7.5 Hz, 4H; CH_2CH$_3$), 2.72–2.77 (q, ^3J(H,H) = 7.5 Hz, 4H; CH_2CH$_3$), 4.12 (s, 4H; 2CH$_2$), 6.20 (s, 1H; CH^{pz}), 7.63 (s, 2H; CH^{Ph}), 8.58 (s, 2H; HC=N), 11.08–11.54 ppm (br; NH); ^{13}C NMR (126 MHz, [D$_6$]DMSO, 301 K): δ = 15.3 (CH_3), 16.4 (*C*H$_2$CH$_3$), 16.7 (*C*H$_2$CH$_3$), 17.2 (CH_3), 19.2 (CH$_3^{Ar}$), 24.3 (br; CH$_2^{py/pz}$), 104.5 (CH^{pz4}), 116.1 (C^q), 117.5 (CH^{Ph}), 118.4 (C^q), 123.1 (C^q), 125.0 (C^q), 133.7 (C^q), 135.5 (C^q), 140.6 (C^q), 141.6 (N=CH), 157.8, 158.0, 158.1, 158.3 ppm (q, J^3(C,F) = 30.8 Hz; TFA); ^{19}F NMR (188 MHz, [D$_6$]DMSO, 301 K): 88.6 ppm (s; C*F*$_3$COO); IR (KBr): $\tilde{\nu}$ = 3436 (m), 3265 (w), 3177 (w), 2965 (m), 2932 (w), 2874 (w), 2359 (w), 1679 (s), 1641 (vs), 1590 (s), 1447 (m), 1385 (m), 1335 (w), 1312 (w), 1264 (s), 1195 (w), 1099 (m), 1017 (m), 866 (w), 802 (vs), 717 cm^{-1} (w); UV/Vis (MeCN/TFA): λ_{max} (ε) = 362 (2.88×10^4 L mol^{-1} cm^{-1}), 435 nm (sh); MS (ESI in MeOH): *m*/*z* (%): 495 (100) [*M*+H]$^+$, 989 (65) [2*M*+H]$^+$, 1102 (61) [2*M*+CF$_3$COOH]$^+$; MS (FAB, 4-NBA): *m*/*z* (%): 495 (100) [*M*]$^+$; HRMS (ESI+, MeOH/H_2O): *m*/*z* calcd for [*M*+H]$^+$: 495.32307; found: 495.32312 [*M*+H]$^+$; elemental analysis calcd (%) for $C_{31}H_{38}N_6$·TFA·1.5 H_2O (635.7): C 62.35, H 6.66, N 13.22; found: C 62.15, H 6.63, N 12.44.

Schiff base macrocycle 4c·TFA: Prepared according to the general procedure for **4**·TFA from **5c** (150 mg, 0.38 mmol) and diaminonaphthaline (97 %) (**12c**) (60.0 mg, 0.38 mmol). Recrystallization from MeOH/Et_2O/CH_2Cl_2 provided **4c**·TFA in the form of a yellow-orange solid (173 mg, 88 %, 0.38 mmolar scale). R_f = 0.57 (aluminum oxide, MeOH/CH_2Cl_2 1:30); m.p. 270–279 °C; ^{1}H NMR (300 MHz, $CDCl_3$, 298 K): δ = 1.03–1.08 (t, ^3J(H,H) = 7.5 Hz, 6H; CH_3), 1.13–1.18 (t, ^3J(H,H) = 7.5 Hz, 6H; CH_3),

2.36–2.43 (q, ^3J(H,H) = 7.5 Hz, 4H; CH_2CH$_3$), 2.57–2.65 (q, ^3J(H,H) = 7.5 Hz, 4H; CH_2CH$_3$), 4.10 (s, 4H; CH$_2$), 6.30 (s, 1H; CH^{pz}), 7.39–7.43 (m, ^3J(H,H) = 3.1 Hz, 2H; CH^{naphtl}), 7.70–7.74 (m, ^3J(H,H) = 3.1 Hz, 4H; CH^{naphtl}), 8.16 (s, 2H; HC=N), 12.23 ppm (brs; NH); ^{13}C NMR (126 MHz, [D$_6$]DMSO, 301 K): δ = 15.3 (*C*H$_2$CH$_3$), 16.4 (*C*H$_2$CH$_3$), 16.7 (CH$_2$*C*H$_3$), 17.3 (CH$_2$*C*H$_3$), 24.4 (br; CH$_2^{py/pz}$), 104.5 (CH^{pz4}), 113.8 (CH^{naphtl}), 123.3 (C^q), 125.4 (CH^{naphtl}), 126.2 (C^q), 127.5 (CH^{naphtl}), 131.6 (C^q), 135.5 (C^q), 141.3 (br; N=CH), 142.9 (C^q), 158.0 ppm (C^q); IR (KBr): $\tilde{\nu}$ = 3422 (w), 3230 (m), 3050 (w), 2960 (m), 2925 (w), 2875 (w), 2354 (w), 1604 (vs), 1433 (s), 1328 (m), 1265 (m), 1222 (m), 1156 (w), 1009 (w), 861 (w), 801 (w), 746 (w), 620 cm^{-1} (w); UV/Vis (CHCl$_3$/0.01 % Et$_3$N): λ_{max} (ε) = 342 (2.44 × 10^4 L mol^{-1} cm^{-1}), 381 nm (sh); UV/Vis (CHCl$_3$/TFA): λ_{max} (ε) = 369 (2.87 × 10^4 L mol^{-1} cm^{-1}), 414 nm (sh); MS (ESI in MeOH): *m*/*z* (%): 517 (100) [*M*+H]$^+$, 1033 (24) [2*M*+H]$^+$, 1069 (40) [2(*M*+H$_2$O)+H]$^+$, 1146 (42) [2*M*+TFA]$^+$; HRMS (ESI+, MeOH/H$_2$O): *m*/*z* calcd for [*M*+H]$^+$: 517.30742; found: 517.30720 [*M*+H]$^+$; MS (FAB, 4-NBA): *m*/*z* (%): 517 (100) [*M*+H]$^+$, 1033 (1) [2*M*+H]$^+$; elemental analysis calcd (%) for C$_{33}$H$_{36}$N$_6$·TFA·H$_2$O (648.7): C 64.80, H 6.06, N 12.96; found: C 64.20, H 6.40, N 12.74.

Schiff base macrocycle 4d·TFA: Prepared according to the general procedure for **4**·TFA from **5c** (104 mg, 0.26 mmol) and 1,3-diaminopropane (99 %) (22.0 μL, 0.26 mmol) and catalyzed by TFA (2 μL, 0.69 mmol, 0.1 equiv). The brown-red solid was purified by means of column chromatography (aluminum oxide, basic, Brockmann activity I, CH$_2$Cl$_2$/MeOH 15:1) to provide **4d**·TFA as a yellow-orange solid (107 mg, 94 %). R_f = 0.38 (aluminum oxide, CH$_2$Cl$_2$/MeOH 20:1); m.p. > 180 °C; ^{1}H NMR (CD$_2$Cl$_2$, 300.13 MHz, 298 K): δ = 0.99–1.05 (t, ^3J(H,H) = 7.5 Hz, 6H; CH$_3$), 1.07–1.12 (t, ^3J(H,H) = 7.5 Hz, 6H; CH$_3$), 1.91 (m, 2H; CH$_2^{prop}$), 2.31–2.38 (q, ^3J(H,H) = 7.5 Hz, 4H; CH_2CH$_3$), 2.46–2.54 (q, ^3J = 7.5 Hz, 4H; CH_2CH$_3$), 3.66–3.71 (m, 4H; CH$_2^{prop}$), 3.84 (s, 4H; 2CH$_2$), 5.53 (s, 1H; CH^{pz}), 7.99 (s, 2H; 2HC=N), 9.46 ppm (NH); ^{13}C NMR (CD$_2$Cl$_2$, 125.77 MHz, 301 K): δ = 16.48 (CH$_3$), 17.4 (*C*H$_2$CH$_3$), 17.7 (*C*H$_2$CH$_3$), 18.6 (CH$_3$), 24.1 (br; CH$_2^{py/pz}$), 30.1 (CH$_2$*C*H$_2$CH$_2$), 34.7, 62.3 (*C*H$_2$CH$_2$*C*H$_2$), 104.3 (CH^{pz4}), 122.4, 124.4, 131.1, 143.5, 150.0 ppm (CH=N); IR (KBr): $\tilde{\nu}$ = 3245 (w), 2947 (s), 1628 (vs), 1443 (s), 1261 (s), 1080 (m), 1020 (m), 801 cm^{-1} (s); UV/Vis (CHCl$_3$/0.01 % Et$_3$N): λ_{max} (ε) = 312 (1.56 × 10^4 L mol^{-1} cm^{-1}), 351 nm (sh); UV/Vis (CHCl$_3$/TFA): λ_{max} (ε) = 325 nm (1.70 × 10^4 L mol^{-1} cm^{-1}); MS (ESI+, MeOH): *m*/*z* (%): 433 (100) [*M*+H]$^+$, 865 (69) [2*M*+H]$^+$; MS (FAB in 4-NBA): *m*/*z* (%): 433 (100) [*M*+H]$^+$; HRMS (ESI+, MeOH/H$_2$O): *m*/*z* calcd for C$_{26}$H$_{36}$N$_6$: 433.30742 [*M*+H]$^+$; found: 433.30731 [*M*+H]$^+$.

Schiff base macrocycle 4e·TFA: Prepared according to the general procedure for **4**·TFA from **5c** (108 mg, 0.27 mmol, 2 equiv) and 1,2,4,5-tetraaminobenzene tetrahydrochloride (**12e**) (38.9 mg, 0.14 mmol, 1 equiv) in dry MeOH (8 mL), and using 5 equiv of TFA (53 μL, 0.69 mmol) and heated at reflux under N$_2$ for 30 h. The brown-red solid was purified by means of column chromatography (aluminum oxide, basic, Brockmann activity I, CH$_2$Cl$_2$/MeOH 20:1) to provide product **4e**·TFA as a violet-brown solid (107 mg, 91 %). R_f = 0.65 (aluminum oxide, MeOH/CH$_2$Cl$_2$ 1:15); m.p. < 290 °C; IR (KBr): $\tilde{\nu}$ = 3375 (w), 3171 (w), 2932 (m), 1631 (vs), 1546 (w), 1443 (m), 1269 (m), 1165 (w), 1010 (s), 957 (w), 796 cm^{-1} (m); UV/Vis (CHCl$_3$/MeOH/0.01 % Et$_3$N): λ_{max} (ε) = 369 (3.06 × 10^4 L mol^{-1} cm^{-1}), 434 nm (sh); UV/Vis (MeOH/TFA): λ_{max} (ε) = 396 (5.02 × 10^4 L mol^{-1} cm^{-1}), 452 nm (sh); MS (ESI in MeOH): *m*/*z* (%): 429 (63) [*M*+2H]$^{2+}$, 856 (100) [*M*+H]$^+$, 1710 (8) [2*M*]$^+$; MS (FAB, in 4-NBA): *m*/*z* (%): 855 (100) [*M*+H]$^+$; HRMS (ESI+, MeOH/H$_2$O): *m*/*z* calcd for C$_{52}$H$_{62}$N$_{12}$: 855.52932 [*M*+H]$^+$, 428.26830 [*M*+2H]$^{2+}$; found: 855.52896 [*M*+H]$^+$, 482.26810 [*M*+2H]$^{2+}$.

Schiff base macrocycle 4f·TFA: Prepared according to the general procedure for **4**·TFA from **5c** (108 mg, 0.20 mmol, 2 equiv) in MeOH (90 mL) and diaminobenzidine (97 %) (**12f**) (21.8 mg, 0.10 mmol, 1 equiv), dissolved in MeOH (2 mL). Recrystallization from MeOH/Et$_2$O at 5 °C gave **4f**·TFA in the form of a red-purple solid (94 mg, 94 %, 0.1 mmolar scale). R_f = 0.56 (aluminum oxide, MeOH/CH$_2$Cl$_2$ 1:15); m.p. 237–239 °C; ^{1}H NMR (500 MHz, [D$_6$]DMSO, 309 K): δ = 1.11–1.19 (m, ^3J(H,H) = 7.5 Hz, 27H; CH$_3$), 2.50 (m, ^3J(H,H) = 7.5 Hz, 8H; CH_2CH$_3$, DMSO), 2.79 (q, ^3J(H,H) = 7.5 Hz, 8H; CH_2CH$_3$), 4.15 (s, 8H; 2CH$_2$), 6.22 (s, 2H; CH^{pz}), 7.75–7.83 (t, 2H; CH^{Ar}), 7.93–7.98 (d, 2H; CH^{Ar}), 8.20 (s, 2H; CH^{Ar}), 8.69 (s, 2H; 2HC=N), 8.82 (s, 2H; 2HC=N), 11.20 (s, 1H; NH), 11.33 ppm (s, 1H; NH); ^{13}C NMR (125.77 MHz, [D$_6$]DMSO, 313 K): δ = 15.1 (CH$_3$), 15.15 (*C*H$_2$CH$_3$), 16.8 (*C*H$_2$CH$_3$), 16.6 (CH$_3$), 16.9, 17.1, 24.2 (br; CH$_2^{py/pz}$), 24.4 (CH$_2^{py/pz}$), 104.6 (CH^{pz4}), 115.7 (CH^{Ar}), 117.3 (CH^{Ar}), 123.0, 123.5 (C^q), 125.0, 125.2, 125.6 (CH^{Ar}), 135.8 (C^q), 136.2 (C^q), 137.5 (C^q), 140.9 (C^q), 142.2 (N=CH), 142.6 (N=CH), 143.3 ppm (C^q); not all signals could be assigned by 2D NMR due to the low solubility of this compound; ^{19}F NMR (188.28 MHz, [D$_6$]DMSO, 298 K): δ = 88.05 ppm (s; CF); IR (KBr): $\tilde{\nu}$ = 3429 (br), 3229 (br), 2955 (w), 2361 (w), 1640 (vs), 1577 (m), 1436 (m), 1322 (w), 1335 (w), 1260 (w), 1188 (w), 1145 (m), 1012 (m), 866 cm^{-1} (m); UV/Vis (CHCl$_3$/0.01 % Et$_3$N): λ_{max} (ε) = 348 (2.39 × 10^4 L mol^{-1} cm^{-1}), 393 nm (sh); UV/Vis (CHCl$_3$/TFA): λ_{max} (ε) = 376 (3.79 × 10^4 L mol^{-1} cm^{-1}), 422 nm (sh); MS (ESI in MeOH): *m*/*z* (%): 467 (48) [*M*+H]$^{2+}$, 931 (100) [*M*+H]$^+$, 954 (7) [*M*+Na]$^+$, 1862 (20) [2*M*+H]$^+$, 1884 (7) [2*M*+Na]$^+$; HRMS (ESI+, MeOH/H$_2$O): *m*/*z* calcd for [*M*+2H]$^{2+}$: 466.28395; found: 466.28388 [*M*+2H]$^{2+}$; MS (FAB, 4-NBA): *m*/*z* (%): 932 (100) [*M*+H]$^+$; elemental analysis calcd (%) for C$_{58}$H$_{66}$N$_{12}$·3TFA·2H$_2$O (1309.3): C 58.71, H 5.62, N 12.84; found: C 58.39, H 5.50, N 12.55.

Schiff base macrocycle 4f·PFS: Prepared according to the general procedure for **4**·TFA from **5c** (108 mg, 0.20 mmol, 2 equiv) in MeOH (90 mL) and diaminobenzidine (97 %) (**12f**) (21.8 mg, 0.10 mmol, 1 equiv), dissolved in MeOH (2 mL), except that 1.0 equiv perfluorosuberic acid (PFS) (96 %) was used to catalyze the condensation. The reaction was heated at reflux for 31 h. The brown-red solid retrieved after rotary evaporation was purified by crystallization in MeOH/Et$_2$O at 5 °C. M.p. 194–211 °C; ^{1}H NMR (500 MHz, [D$_6$]DMSO, 309 K): δ = 1.13–1.20 (m, ^3J(H,H) = 7.5 Hz, 27H; CH$_3$), 2.50 (m, ^3J(H,H) = 7.5 Hz, 8H; CH_2CH$_3$, DMSO), 2.79 (q, ^3J(H,H) = 7.5 Hz; 8H; CH_2CH$_3$), 3.40 (brs; H$_2$O), 4.14 (s, 4H; 2CH$_2$), 4.15 (s, 4H; 2CH$_2$), 6.22 (s, 2H; CH^{pz}), 7.73–7.75 (d, 2H; CH^{Ar}), 7.92–7.93 (d, 2H; CH^{Ar}), 8.19 (s, 2H; CH^{Ar}), 8.67 (s, 2H; 2HC=N), 8.79 (s, 2H; 2HC=N), 11.13 (s, 1H; NH), 11.27 ppm (s, 1H; NH); ^{13}C NMR (125.77 MHz, [D$_6$]DMSO, 313 K): δ = 15.1, 15.2 (CH$_3$), 16.1, 16.4, 16.7 (*C*H$_2$CH$_3$), 17.0, 17.1(CH$_3$), 24.3 (br; CH$_2^{py/pz}$), 104.6 (CH^{pz}), 109.2, 115.0, 117.2 (CH^{Ar}), 123.1, 123.5 (C^q), 125.0, 125.1, 125.2, 125.6 (CH^{Ar}), 126.9, 135.8 (C^q), 136.1 (C^q), 137.5 (C^q), 142.2, 142.6 (N=CH), 158.2 ppm (CF$_2$); ^{19}F NMR (188.29 MHz, [D$_6$]DMSO, 298 K): δ = 41.1–41.4 (dd; CF$_2$), 48.0 ppm (s; CF$_2$); IR (KBr): $\tilde{\nu}$ = 3208 (br), 2964 (m), 2930 (w), 2871 (w), 1679 (vs), 1636 (vs), 1582 (w), 1552 (w), 1439 (m), 1377 (w), 1323 (w), 1199 (s), 1139 (w), 1061 (w), 1007 (s), 958 (w), 804 cm^{-1} (br); UV/Vis (MeOH/Et$_3$N): λ_{max} (ε) = 352 (2.44 × 10^4 L mol^{-1} cm^{-1}), 390 nm (sh); UV/Vis (MeOH/PFS): λ_{max} (ε) = 380 (2.93 × 10^4 L mol^{-1} cm^{-1}), 458 nm (sh); MS (ESI in MeOH): *m*/*z* (%): 467 (100) [*M*+2H]$^{2+}$, 931 (7) [*M*+H]$^+$; elemental analysis calcd (%) for C$_{58}$H$_{66}$N$_{12}$·C$_8$F$_{12}$O$_4$H$_2$·2H$_2$O (1357.4): C 58.40, H 5.35, N 12.38; found: C 57.93, H 5.34, N 12.15.

X-ray crystallography: Single crystals of **9**·0.5 THF were grown from solutions in THF/Et$_2$O/light petroleum, those of **4a** were grown at 5 °C from a saturated ethanolic solution, crystals of the TFA salt **4a**·TFA were obtained by slow evaporation of a saturated solution in MeOH/CH$_2$Cl$_2$. Diffraction-grade crystals of **4b**·TFA·H$_2$O and **4c**·TFA·H$_2$O formed upon slow evaporation of solutions of MeOH/CH$_2$Cl$_2$.

X-ray data were collected on a STOE IPDS II diffractometer (graphite monochromated Mo$_{K\alpha}$ radiation, λ = 0.71073 Å) by use of ω scans. The structures were solved by direct methods and refined on F^2 using all reflections with SHELX-97.[27] All non-hydrogen atoms except those in the disordered parts of **9**·0.5 THF were refined anisotropically. Hydrogen atoms which were not involved in hydrogen bonding were placed in calculated positions and assigned to an isotropic displacement parameter of 0.08 Å^2. The positional parameters of all nitrogen- and oxygen-bound hydrogen atoms in **4b**·TFA·H$_2$O and **4c**·TFA·H$_2$O were refined by using DFIX and DANG restraints. Their isotropic displacement parameters were refined freely. The pyrrole ring in **9** as well as the F$_3$C group of the CF$_3$COO$^-$ anion in **4c**·TFA·H$_2$O were disordered about two positions (occupancy factors: **9**·0.5 THF, 0.53(2)/0.47(2); **4c**·TFA·H$_2$O, 0.925(5)/0.075(5)). In both cases SADI restraints were used to model the disorder. Additionally a THF solvent molecule in **9**·0.5 THF was found to be disordered about a center of inversion and was refined with a fixed occupancy

Table 1. Crystal data and refinement details for **9**·0.5 THF, **4b**·TFA·H_2O, and **4c**·TFA·H_2O.

	9·0.5 THF	**4b**·TFA·H_2O	**4c**·TFA·H_2O
empirical formula	$C_{16}H_{22}ClN_3O_{1.5}$	$C_{33}H_{41}F_3N_6O_3$	$C_{35}H_{39}F_3N_6O_3$
M_r	315.82	626.72	648.72
crystal size [mm]	$0.32\times0.24\times0.16$	$0.20\times0.15\times0.08$	$0.29\times0.20\times0.06$
crystal system	monoclinic	triclinic	triclinic
space group	$P2_1/c$ (no. 14)	$P\bar{1}$ (no. 2)	$P\bar{1}$ (no. 2)
a [Å]	11.3641(15)	9.2223(9)	9.2295(16)
b [Å]	17.068(2)	12.0717(12)	11.894(2)
c [Å]	8.4097(11)	15.0175(15)	14.983(3)
α [°]	90	66.062(7)	104.052(13)
β [°]	97.179(11)	87.286(8)	98.876(13)
γ [°]	90	83.853(8)	91.087(14)
V [Å^3]	1618.4(4)	1519.3(3)	1573.8(5)
Z	4	2	2
ρ_{calcd} [g cm^{-3}]	1.296	1.370	1.369
$F(000)$	672	664	684
μ [mm^{-1}]	0.243	0.102	0.101
T_{max}/T_{min}	–	0.9797/0.8444	0.9797/0.8444
hkl range	−12 to 13, ±19, −9 to 7	±10, ±14, −17 to 16	±10, −14 to 13, −17 to 14
θ range [°]	1.81–24.00	1.48–24.84	1.77–24.83
measured reflections	11 050	15 739	11 129
unique reflections [R_{int}]	2498 [0.1111]	5210 [0.0754]	5082 [0.1100]
observed reflections ($I>2\sigma(I)$)	1688	3234	2393
refined parameters	188	436	462
restraints	6	3	38
goodness-of-fit	1.025	1.017	1.006
$R1$ ($I>2\sigma(I)$)	0.0878	0.0617	0.0716
$wR2$ (all data)	0.2318	0.1531	0.1348
residual electron density [e Å^{-3}]	−0.464/0.504	−0.335/0.399	−0.221/0.249

factor of 0.5. Face-indexed absorption corrections for **4b**·TFA·H_2O and **4c**·TFA·H_2O were performed numerically with the program X-RED.[28] Table 1 contains the crystal data and refinement details for **9**·0.5 THF, **4b**·TFA·H_2O, and **4c**·TFA·H_2O.

CCDC-666276 (**9**·0.5 THF), CCDC-666277 (**4b**·TFA·H_2O), and CCDC-666278 (**4c**·TFA·H_2O) contain the supplementary crystallographic data for this paper. These data can be obtained free of charge from The Cambridge Crystallographic Data Centre via www.ccdc.cam.ac.uk/data_request/cif.

Acknowledgements

We thank the Deutsche Akademische Austauschdienst (DAAD, PPP USA program) and the US National Science Foundation (NSF-INT 0321652 and NSF-CHE 0517782) for support. We thank Michelle L. Dean and Andreas Schwarz for help in the preparation of the building blocks.

[1] a) A. Asat, D. Dolphin, *Chem. Rev.* **1997**, *97*, 2267–2340; b) J. L. Sessler, S. Weghorn, *Expanded, Contracted & Isomeric Porphyrins*, Pergamon, New York, **1997**; c) W. A. Reiter, A. Gerges, S. Lee, T. Deffo, T. Clifford, A. Danby, K. Bowman-James, *Coord. Chem. Rev.* **1998**, *174*, 343–359.

[2] a) *The Supramolecular Chemistry of Anions* (Eds.: A. Bianchi, K. Bowman-James, E. Garcia-España), Wiley, New York, **1997**; b) J. L. Sessler, S. Camiolo, P. A. Gale, *Coord. Chem. Rev.* **2003**, *240*, 17–55; c) W.-S. Cho, J. L. Sessler, in *Functional Synthetic Receptors* (Eds.: T. Schrader, A. D. Hamilton), Wiley-VCH, Weinheim, **2005**, 165–256; d) J. L. Sessler, P. A. Gale, W.-S. Cho, *Anion Receptor Chemistry (Monographs in Supramolecular Chemistry)* (Ed.: J. F. Stoddart), Royal Society of Chemistry, Cambridge, **2006**; e) M. A. Palacios, R. Nishiyabu, M. Marquez, P. Anzensbacher, Jr., *J. Am. Chem. Soc.* **2007**, *129*, 7538–7544.

[3] Reviews: Schiff base macrocycles: a) P. A. Vigato, S. Tamburini, *Coord. Chem. Rev.* **2004**, *248*, 1717–2128; b) N. E. Borisova, M. D. Reshetova, Y. A. Ustynyuk, *Chem. Rev.* **2007**, *107*, 46–79; Porphocyanines: c) L. Y. Xie, R. W. Boyle, D. Dolphin, *J. Am. Chem. Soc.* **1996**, *118*, 4853–4859.

[4] Reviews concerning texaphyrins: a) J. L. Sessler, G. Hemmi, T. D. Mody, T. Murai, A. Burrell, S. W. Young, *Acc. Chem. Res.* **1994**, *27*, 43–50; b) J. L. Sessler, V. Kral, M. C. Hoehner, K. O. A. Chin, R. Davila, *Pure Appl. Chem.* **1996**, *68*, 1291–1295.

[5] Select examples of other cyclic and acyclic pyrrole-based Schiff base compounds: a) F. V. Acholla, F. Takusagawa, K. B. Mertes, *J. Am. Chem. Soc.* **1985**, *107*, 6902–6908; b) J. B. Love, A. J. Blake, C. Wilson, S. D. Reid, A. Novak, P. B. Hitchcock, *Chem. Commun.* **2003**, 1682–1683; c) Z. Wu, Q. Chen, S. Xiong, B. Xin, Z. Zao, L. Jiang, J. S. Ma, *Angew. Chem.* **2003**, *115*, 3393–3396; *Angew. Chem. Int. Ed.* **2003**, *42*, 3271–3274; d) J. M. Veauthier, E. Tomat, V. M. Lynch, J. L. Sessler, U. Mirsaidov, J. T. Markert, *Inorg. Chem.* **2005**, *44*, 6736–6743.

[6] a) G. Givaja, A. J. Blake, C. Wilson, M. Schröder, J. B. Love, *Chem. Commun.* **2003**, 2508–2509; b) G. Givaja, M. Volpe, J. W. Leeland, M. A. Edwards, T. K. Young, S. B. Darby, S. D. Reid, A. J. Blake, C. Wilson, J. Wolowska, E. J. L. McInnes, M. Schröder, J. B. Love, *Chem. Eur. J.* **2007**, *13*, 3707–3723.

[7] a) E. A. Katayev, Y. A. Ustynyuk, V. M. Lynch, J. L. Sessler, *Chem. Commun.* **2006**, 4682–4684; b) E. A. Katayev, N. V. Boev, V. N. Khrustalev, Y. A. Ustynyuk, I. G. Tananaev, J. L. Sessler, *J. Org. Chem.* **2007**, *72*, 2886–2896.

[8] a) V. J. Arán, M. Kumar, J. Molina, L. Lamarque, P. Navarro, E. García-España, J. A. Ramírez, S. V. Luis, B. Escuder, *J. Org. Chem.* **1999**, *64*, 6135–6146; b) L. Lamarque, P. Navarro, C. Miranda, V. J. Arán, C. Ochoa, F. Escartí, E. García-España, J. Latorre, S. V. Luis, J. F. Miravet, *J. Am. Chem. Soc.* **2001**, *123*, 10560–10570; c) C. Miranda, F. Escarti, L. Lamarque, M. J. R. Yunta, P. Navarro, E. García-España, M. L. Jimeno, *J. Am. Chem. Soc.* **2004**, *126*, 823–833; d) C. Miranda, F. Escarti, L. Lamarque, E. García-España, M. J. R. Yunta, P. Navarro, J. Latorre, F. Lloret, H. R. Jiménez, M. J. R. Yunta, *Eur. J. Inorg. Chem.* **2005**, 189–208; e) A. Doménech, E. García-España, P. Navarro, C. Miranda, *Dalton Trans.* **2006**, 4926–4935.

[9] a) J. Elguero, in *Comprehensive Heterocyclic Chemistry II: A Review of the Literature 1982–1995, Vol. 3* (Eds.: A. R. Katritzky, C. V. Rees, E. F. V. Scriven), Elsevier, Oxford, **1996**; b) C. Foces-Foces, A. Echevarría, N. Jagerovic, I. Alkort, J. Elguero, U. Langer, O. Klein, M. Minguet-Bonvehí, H.-H. Limbach, *J. Am. Chem. Soc.* **2001**, *123*, 7898–7906; c) A. Sachse, L. Penkova, G. Noel, S. Dechert, O. A. Varzatskii, I. O. Fritsky, F. Meyer, *Synthesis* **2008**, 800–806.

[10] a) Th. A. Kaden, *Coord. Chem. Rev.* **1999**, *190*, 371–389; b) R. Mukherjee, *Coord. Chem. Rev.* **2000**, *203*, 151–218; c) F. Meyer, *Eur. J. Inorg. Chem.* **2006**, 3789–3800.

[11] Examples include the following: a) T. Kamiusuki, H. Ōkawa, N. Matsumoto, S. Kida, *J. Chem. Soc. Dalton Trans.* **1990**, 195–198;

b) M. Raidt, L. Siegfried, T. A. Kaden, *Dalton Trans.* **2003**, 4493–4497; c) A. Eisenwiener, M. Neuburger, Th. A. Kaden, *Dalton Trans.* **2007**, 218–233; d) J.-H. Liu, X.-Y. Wu, Q.-Z. Zhang, X. He, W.-B. Yang, C.-Z. Lu, *J. Coord. Chem.* **2007**, *60*, 1373–1379.

[12] a) F. Meyer, S. Beyreuther, K. Heinze, L. Zsolnai, *Chem. Ber./Recueil* **1997**, *130*, 605–613; b) F. Meyer, K. Heinze, B. Nuber, L. Zsolnai, *J. Chem. Soc. Dalton Trans.* **1998**, 207–217; c) F. Meyer, E. Kaifer, P. Kircher, K. Heinze, H. Pritzkow, *Chem. Eur. J.* **1999**, *5*, 1617–1630; d) M. Konrad, F. Meyer, A. Jacobi, P. Kircher, P. Rutsch, L. Zsolnai, *Inorg. Chem.* **1999**, *38*, 4559–4566; e) M. Konrad, S. Wuthe, F. Meyer, E. Kaifer, *Eur. J. Inorg. Chem.* **2001**, 2233–2240; f) J. Ackermann, F. Meyer, E. Kaifer, H. Pritzkow, *Chem. Eur. J.* **2002**, *8*, 247–258; g) J. Ackermann, F. Meyer, H. Pritzkow, *Inorg. Chim. Acta* **2004**, *357*, 3703–3711; h) B. Bauer-Siebenlist, F. Meyer, E. Farkas, D. Vidovic, J. A. C. Seijo, R. Herbst-Irmer, H. Pritzkow, *Inorg. Chem.* **2004**, *43*, 4189–4202; i) B. Bauer-Siebenlist, F. Meyer, E. Farkas, D. Vidovic, S. Dechert, *Chem. Eur. J.* **2005**, *11*, 4349–4360; j) G. Noël, J. C. Röder, S. Dechert, H. Pritzkow, L. Bolk, S. Mecking, F. Meyer, *Adv. Synth. Catal.* **2006**, *348*, 887–897; k) A. Prokofieva, A. I. Prikhod'ko, E. A. Enyedy, E. Farkas, W. Maringgele, S. Demeshko, S. Dechert, F. Meyer, *Inorg. Chem.* **2007**, *46*, 4298–4307; l) J. Ackermann, S. Buchler, F. Meyer, *C. R. Chim.* **2007**, *10*, 421–432.

[13] S. Katsiaouni, S. Dechert, C. Brückner, F. Meyer, *Chem. Commun.* **2007**, 951–953.

[14] E. Lind, PhD Thesis, Michigan State University, East Lansing, MI (USA), **1987**.

[15] J. C. Röder, F. Meyer, M. Konrad, S. Sandhöfner, E. Kaifer, H. Pritzkow, *Eur. J. Org. Chem.* **2001**, 4479–4487.

[16] T. G. Schenck, J. M. Downes, C. R. C. Milne, P. B. MacKenzie, H. Boucher, J. Whelan, B. Bosnich, *Inorg. Chem.* **1985**, *24*, 2334–2337.

[17] J. C. Röder, F. Meyer, H. Pritzkow, *Organometallics* **2001**, *20*, 811–817.

[18] S. Buchler, F. Meyer, E. Kaifer, H. Pritzkow, *Inorg. Chim. Acta* **2002**, *337*, 371–386.

[19] a) J. C. Röder, F. Meyer, E. Kaifer, *J. Organomet. Chem.* **2002**, *641*, 113–120; b) T. Sheng, S. Dechert, I. Hyla-Kryspin, R. F. Winter, F. Meyer, *Inorg. Chem.* **2005**, *44*, 3863–3874; c) T. Sheng, S. Dechert, A. C. Stückl, F. Meyer, *Eur. J. Inorg. Chem.* **2005**, 1293–1302.

[20] a) C. Brückner, E. D. Sternberg, R. W. Boyle, D. Dolphin, *Chem. Commun.* **1997**, 1689–1690; b) J.-W. Ka, C.-H. Lee, *Tetrahedron Lett.* **2000**, *41*, 4609–4613; c) W. Jiao, T. D. Lash, *J. Org. Chem.* **2003**, *68*, 3896–3901.

[21] a) R. Chong, P. S. Clezy, A. J. Liepa, A. W. Nichol, *Aust. J. Chem.* **1969**, *22*, 229–238; b) W.-H. Wei, Z. Wang, T. Mizuno, C. Cortez, L. Fu, M. Sirisawad, L. Naumovski, D. Magda, J. L. Sessler, *Dalton Trans.* **2006**, 1934–1942.

[22] a) J. L. Sessler, T. Murai, V. Lynch, M. Cyr, *J. Am. Chem. Soc.* **1988**, *110*, 5586–5588; b) S. Hannah, V. M. Lynch, N. Gerasimchuk, D. Magda, J. L. Sessler, *Org. Lett.* **2001**, *3*, 3911–3914.

[23] a) J. L. Hughey IV, S. Knapp, H. Schugar, *Synthesis* **1980**, 489–490; b) H. Firouzababi, E. Ghaderi, *Tetrahedron Lett.* **1978**, *19*, 839–840.

[24] a) R. Charriere, T. A. Jenny, H. Rexhausen, A. Gossauer, *Heterocycles* **1993**, *36*, 1561–1575; b) A. Srinivasan, T. Ishizuka, A. Osuka, H. Furuta, *J. Am. Chem. Soc.* **2003**, *125*, 878–879; c) M. Suzuki, M.-C. Yoon, D. Y. Kim, J. H. Kwon, H. Furuta, D. Kim, A. Osuka, *Chem. Eur. J.* **2006**, *12*, 1754–1759.

[25] a) G. D. Hartman, L. M. Weinstock, *Org. Synth.* **1988**, 620; b) J. L. Sessler, A. Mozaffari, M. R. Johnson, *Org. Synth.* **1992**, *70*, 68–78.

[26] R. P. Briñas, C. Brückner, *Tetrahedron* **2002**, *58*, 4375–4381.

[27] G. M. Sheldrick, SHELX97, Programs for Crystal Structure Analysis (release 97-2), Universität Göttingen, Germany, **1998**; G. M. Sheldrick, *Acta Cryst. A* **2008**, *64*, 112–122.

[28] STOE & CIE GmbH, X-RED, Darmstadt, Germany, **2002**.

Received: November 9, 2007
Published online: April 17, 2008

